OPTIMIZATION AND SENSITIVITY ANALYSIS OF FOAM ASSISTED WATER ALTERNATING GAS

BY

NAJMUDEEN SIBAWEIHI

A Thesis Presented to the

DEANSHIP OF GRADUATE STUDIES

KING FAHD UNIVERSITY OF PETROLEUM & MINERALS

DHAHRAN, SAUDI ARABIA

In Partial Fulfillment of the

Requirements for the Degree of

MASTER OF SCIENCE

In

PETROLEUM ENGINEERING

JUNE, 2013

KING FAHD UNIVERSITY OF PETROLEUM & MINERALS
DHAHRAN 31261, SAUDI ARABIA

DEANSHIP OF GRADUATE STUDIES

This thesis, written by **NAJMUDEEN SIBAWEIHI** under the direction of his thesis adviser and approved by his thesis committee, has been presented to and accepted by the Dean of Graduate Studies, in partial fulfillment of the requirements for the degree of **MASTER OF SCIENCE IN PETROLEUM ENGINERING**.

Thesis Committee

Dr. Abeeb A. Awotunde (Adviser)

Dr. Hasan Y. Al-Yousef (Member)

Dr. Abdullah S. Sultan (Member)

for Dr. Abdullah S. Sultan
Department Chairman

Dr. Salam A. Zummo
Dean of Graduate Studies

1/7/13
Date

Dedication

This thesis is dedicated to my parents and siblings.

ACKNOWLEDGMENTS

My sincere gratitude goes to Almighty Allah (SWT) who I do not thank anyone more than him for his guidance and blessing bestowed upon me. My appreciation also goes to King Fahd University of Petroleum & Minerals for providing me the scholarship as Research Assistant to pursue graduate studies in Petroleum Engineering. My sincere appreciation goes to Dr. Abdul-Aziz Al-Majed and Dr. Abdullah S. Sultan, past and current chair of Petroleum Engineering Department respectively for their support and guidance throughout my stay at the department. I also express my sincere appreciation to my thesis advisor Dr. Abeeb A. Awotunde for his guidance and support throughout my research work.

I am also highly grateful to my thesis committee members Dr. Hasan Al-Yousef and Dr. Abdullah S. Sultan for their guidance, suggestion and support throughout my research work.

I would like to extend my appreciation to my cousin Musah Muhydeen, Ghanaian community in Dhahran especially, Dr. Robert, Dr. Issaka, Abdul-Samed, Abdul-Rashid, Malik, Kamal, Eric, Nester etc. My appreciation also goes to my friends Moshood, Maganda, Amin, Buhari and Talley Fogang.

I would like to thank my family for the support given me all my life.

TABLE OF CONTENTS

LIST OF TABLES

LIST OF FIGURES

THESIS ABSTRACT

NAME: Najmudeen Sibaweihi

TITLE OF STUDY: Optimization and Sensitivity Analysis of Foam Assisted Water Alternating Gas

MAJOR FIELD: Petroleum Enginering

DATE OF DEGREE: June,2013

Optimization of CO_2 foam flooding has been investigated over the years using mainly experimental and manually changing of parameters in the simulator. Genetic Algorithm (GA) and Differential Evolution (DE) have been implemented in optimizing CO_2 flooding as the optimizer of the objective function. GA is very popular in the petroleum industry for optimization. GA main disadvantages are that it is computationally expensive and not good optimizer as compared to recent developed algorithms.

In this study, we implemented Covariance Matrix Adaptation Evolution Strategy (CMA-ES) and Differential Evolution (DE) to optimize CO_2 foam flooding. These algorithms are newly developed algorithms that require less simulation runs as compared to GA. The objective was to optimize Net Present Value (NPV).

MATLAB was used as objective function optimizer and Schlumberger ECLIPSE-100 as objective function evaluator.

A concept of well placement optimization which incorporates minimum inter-well distance has been developed. The optimum ratio of length of time for water injection to length of time for gas injection is between 0.5 and 1 at constant injection rate. Lower ratios below 0.5 have higher recovery at early stage of foam project but efficiency decreases at later stage since below 0.5 ratio is closer to continuous foam flooding.

ملخص الرسالة

الاسم الكامل: نجم الدين سيباويه

عنوان الرسالة: تحليل الأمثلية والحساسية للرغوة المعززة للماء المتناوب مع الغاز

التخصص: هندسة البترول

تاريخ الدرجة العلمية: يونيو 2013

تمت دراسة الغمر برغوة ثاني أكسيد الكربون كطريقة للاستخلاص المحسن للنفط على مدى السنوات الماضية والطريقة المثلى للحقن بشكل تجريبي و يدوي عن طريق تغيير المتغيرات في المحاكي. وقد طُبقت كل من الخوارزميات الجينية (GA) والتطور التفاضلي (DE) في أمثلية الغمر بثاني أكسيد الكربون كمحسن لدالة الهدف. و تعتبر الخوارزميات الجينية أكثر استخداما للأمثلية في الصناعات البترولية على أن مساوئ الخوارزميات الجينية الجوهرية هي أنها مكلفة حسابيا وكذلك ليست محسنة جيدة مقارنة مع الخوارزميات المطورة حديثاً.

تم في مشروع هذه الرسالة تنفيذ كل من استراتيجية تطوير وتعديل المصفوفة المتغايرة (CMA-ES) والتطور التفاضلي (DE) لتحسين الغمر برغوة ثاني أكسد الكربون. هذه الخوارزميات طُورت حديثا بحيث تتطلب أقل عمليات تشغيل للمحاكاة مقارنة مع الخوارزميات الجينية. إن الهدف كان لتحسين صافي القيمة الحالية (NPV). وقد تم استخدام كل من برنامجي الماتلاب (Matlab) كمُحسِّن دالة الهدف وبرنامج المحاكاة الايكلبس (Eclipse) المطور من قبل شلمبرجر كمُقيِّم لدالة الهدف.

تم تطوير مفهوم جديد لأمثلية موضع البئر في المكامن النفطية بحيث يتضمن على أقل مسافة بين بئرين. إن النسبة المثلى لطول الفترة الزمنية لحقن الماء إلى طول الفترة الزمنية لحقن الغاز كانت ما بين 0.5 و 1 في حالة الحقن الثابت. وقد تمت ملاحظة انه و في حالة النسب المنخفضة التي أقل من 0.5، كان الاستخلاص أعلى في مرحلة مبكرة من مشروع الرغوة، لكن بعد ذلك انخفضت الكفاءة لأن النسبة أقل من 0.5 أصبحت قريبة من الغمر بالرغوة المستمر.

CHAPTER 1

INTRODUCTION

1.1 Background

Over the years CO_2 flooding in mature fields has proven to be an important enhanced oil recovery method. The increasing number of mature fields across the world demands new ways of recovering the residual oil. Injection of CO_2 at supercritical pressure to displace the immobile oil to producing zone can also serve as a means of reducing the amount of CO_2 in the atmosphere by capturing and sequestering in the mature reservoirs.

To increase recovery by CO_2 flooding, the injected CO_2 swells the oil, reduces IFT, reduces the viscosity of oil, reduces the density of oil and vaporizes the oil (Mungan, 1981). Application of CO_2 flooding as means of enhanced recovery has its challenges, which various investigators have tried to solve over the decades. The common challenges of CO_2 flooding are gravity segregation, reservoir heterogeneity and high mobility ratio of CO_2 oil systems (Bai et al., 2005). These cause

a reduction in macroscopic sweep efficiency even though the microscopic efficiency sweep efficiency may be high.

To solve the challenge of high mobility ratio, early breakthrough and to reduce the of amount of CO_2 utilized in producing per barrel, Water Alternating Gas (WAG), Surfactant Alternating Gas (SAG), Foam Assisted Water Alternating Gas (FAWAG) are examples of injection methods which have been studied in laboratory and implemented in the field (Skauge et al., 2002; Grigg and Mikhalin, 2007; Kloet et al., 2009). In SAG and FAWAG modes of injection, foam is injected alternately with gas to control the mobility of gas and reduce the interfacial tension between oil and water. Optimizing the parameters of these injectivity modes can lead to maximizing NPV by reducing the amount of CO_2 utilized in producing per barrel of crude oil and improvement of sweep efficiency (Chen et al., 2009). GA has been the main algorithm which has been applied in optimizing CO_2 flooding (Chen et al., 2009). Differential Evolution (DE) also has been applied to optimize CO_2 flooding during sequestration and EOR (Jahangiri and Zhang, 2011).

1.2 Statement of the Problem

Optimization of foam flooding parameters is very important for successful field or laboratory application. Over the years, optimization of CO_2-foam flooding has been implemented by manually changing some parameters (sensitivity studies) in simulator input files (Kloet et al., 2009). Stochastic optimization algorithms have been shown to be successful in optimization of engineering problems. These algorithms automate the optimization procedure with advantage of multiple simulation runs which quality maps and manual optimization processes are deficient in.

1.3 Objectives

- To conduct sensitivity study and determine the effects of cycle length of FAWAG, cycle ratio of FAWAG, and amount of surfactant on recovery performance.

- To study the performance of two stochastic optimization algorithm on optimizing the parameters of FAWAG such as well placement and ratio of length of time of water injection to length of time of gas injection that maximizes NPV.

CHAPTER 2

LITERATURE REVIEW

2.1 CO_2 Flooding

Exploitation of oil from petroleum reservoirs is in three main stages; primary, secondary and tertiary recovery stages. In primary recovery, the reservoir uses its own natural energy to produce the oil to the surface. For the secondary and tertiary stage, the reservoir needs an external energy to produce the remaining oil in its pores. In primary production, the recovery range for oil production is between $5 - 15\%$ OOIP and secondary recovery can add an additional $20 - 40\%$ OOIP (Enick et al., 2012). To displace the remaining oil in the pores, various methods have been used in laboratory, numerical simulation and field application after primary production. In EOR, what we seek to do is to reduce the residual oil saturation at abandonment of the field. Waterflooding, surfactant flooding, surfactant polymer, nitrogen flooding and CO_2 flooding are some of the EOR methods which have been applied to produce additional oil after primary recovery.

In this study, the focus is on CO_2 EOR method.

In recent times global warming effect has lead to the need to reduce the amount of CO_2 in the atmosphere. In turn, this has lead to an increase in the use of atmospheric CO_2 for EOR. Capturing and sequestration of CO_2 into saline aquifers and abandoned petroleum reservoirs have gradually evolved into a field of research (Ghomian et al., 2008). In the past, CO_2 sequestration and EOR have been applied in petroleum reservoirs as independent objectives. That is sequestration is applied to mature or abandoned petroleum reservoirs for storage purpose and EOR is applied at the secondary and tertiary stages for incremental recovery. In the past decade, several researchers have investigated joint EOR and Sequestration (Ghomian et al., 2008). In the joint EOR and sequestration, the revenue from the incremental oil recovery serves as means of cost reduction for sequestration and with more CO_2 sequestered the operating companies can claim carbon credit.

To increase recovery by CO_2 flooding, the injected CO_2 swells the oil, reduces IFT, reduces the viscosity of oil, reduces the density of oil and vaporizes the oil (Mungan, 1981). To displace the oil in the pores, the injected CO_2 must be less mobile than the immobile oil in the reservoir for efficient displacement. CO_2 flooding is broadly categorized into two methods; miscible flooding and immiscible flooding (Wang et al., 2008). The main challenges in CO_2 flooding are gravity segregation, reservoir heterogeneity and high mobility ratio of CO_2. These cause a reduction in macroscopic sweep efficiency even though the microscopic sweep efficiency may be high.

2.2 Miscible CO_2 Flooding

In miscible CO_2 flooding, the pressure of the injected CO_2 must be above the Minimum Miscibility Pressure (MMP). MMP is defined as the minimum pressure at which CO_2 form a single phase with oil (Yongmao et al., 2004). MMP is affected by reservoir temperature, amount of impurities (CH_4 and N_2) in the CO_2 and composition of crude oil (Arshad et al., 2009). When the injection pressure of CO_2 is equal or above the MMP, CO_2 completely mixes with oil to form a single phase and this is referred to as first contact miscibility (Shedid et al., 2008). Usually CO_2 becomes miscible with reservoir oil after multiple contacts and is referred to as multiple contact miscibility (Almehaideb et al., 2008; Arshad et al., 2009). Miscible CO_2 flooding or near miscible CO_2 flooding has been applied in most Permian Basin CO_2 EOR projects (Zhou et al., 2012). Reservoirs which qualify for CO_2 miscible flooding have API gravity greater than 30 - 36 corresponding to CO_2 density of 0.876 g/ml and 0.922 g/ml respectively (Enick et al., 2012). The fracturing pressure of the formation must be higher than the MMP for a reservoir to qualify for miscible flooding. The typical range of depth for miscible flooding ranges from $3000 - 7000$ ft (Enick et al., 2012). Recovery factor for miscible flooding ranges between $10 - 20\%$ (Enick et al., 2012). MMP requirements for N_2 and CH_4 are higher than that for CO_2 this makes CO_2 miscible flooding more efficient (Wang et al., 2008). Viscous, capillary, diffusive and gravity forces are the major controlling factors during the transport and recovery of oil during miscible CO_2 flooding in fractured reservoirs (Asghari and Torabi, 2008). The reduction

of residual oil under miscible conditions is due to reduction of IFT between CO_2 and residual oil (Ghedan, 2009). For successful implementation of miscible CO_2 flooding, the following criteria have to be met by the candidate reservoir (Gao et al., 2010);

- The reservoir should have demonstrated good response to waterflood.
- The recovery factor after waterflood should be greater than 20%: but less than 50 of the OOIP.
- The reservoir depth must be greater than 2500 ft.
- The API gravity of the oil should be greater than 27^oAPI.
- The viscosity of the oil should be less than 10 cp at reservoir conditions.
- Reservoir porosity and effective permeability should be greater than 12% and 10 mD respectively.

2.3 Modes of CO_2 Injection

Different modes of injection of CO_2 have been investigated both in laboratory (Zuta and Fjelde, 2011) and by numerical simulation (Mirkalaei et al., 2011) studies. Some of these have been successfully applied in the laboratory but have not gained significant applications in the field due to operational challenges.

2.3.1 Continuous Gas Injection

Continuous Gas Injection (CGI) is one of the methods with both successful laboratory and field applications. In CGI, CO_2 gas is injected continuously into the reservoir. CGI is suitable for gravity drainage reservoirs and reservoir where waterflooding application is inefficient (Zhou et al., 2012). At early stage of CGI application in the field, higher recoveries are recorded which affect the project economics positively (Zhou et al., 2012). Miscible CGI investigations in the laboratory have proven to be effective in recovering residual oil after waterflooding of petroleum reservoirs (Mungan, 1981). Due to its main challenge of early CO_2 breakthrough, high CO_2 recycling, higher cumulative net utilization factor the management and operations is arduous (Zhou et al., 2012).

2.3.2 Water Alternating Gas Injection

Water Alternating Gas (WAG) injection has been applied as one of the injection modes to solve the challenges of CGI method. In WAG, CO_2 is injected alternately with water. WAG's ability to improve macroscopic displacement efficiency by water and microscopic efficiency by gas makes it more efficient than CGI (Guzman et al., 1994; Mirkalaei et al., 2011). WAG has more favorable gas-oil mobility ratio, controls early breakthrough and maintains reservoir pressure. This gives it advantage over CGI (Wang et al., 2008). In WAG, the water is used as medium for control of gas mobility and displacement front (Mirkalaei et al., 2011). WAG has been demonstrated in both simulation and pilot test as effective in increasing

recovery from low permeability reservoirs (Guo et al., 2006). Economic benefits of WAG injection scheme is improved due to reduction in volume of the amount of CO_2 injected in the reservoir (Chen et al., 2009; Ghomian et al., 2008). A change in the composition of the resident fluid as the oil swells during the gas injection stage of WAG leading to changes in the density and viscosity of resident oil. These changes in the properties of the oil give rise to additional recovery (Mirkalaei et al., 2011). In WAG, the injected water sweeps any oil mobilized due to improve miscibility (Odi and Gupta, 2010). Due to its operational flexibility and conformance control, 90% of CO_2 projects in US use either WAG or Tapered Water Alternating Gas (Zhou et al., 2012).

Performance of WAG injection is affected by heterogeneity, wettability, fluid properties, miscibility conditions, trapped gas, injection techniques and well operational parameters (Jiang et al., 2012; Mirkalaei et al., 2011). WAG is not applicable in water sensitive reservoirs or tight reservoirs (Enick et al., 2012). Incremental recovery of WAG in carbonate reservoirs ranges between $8 - 25\%$ of OOIP after about $40 - 60\%$ HCPV CO_2 is injected (Zhou et al., 2012). For effective mobility control of gas in WAG process, CO_2 soluble surfactants have been designed to be dissolved in the injected CO_2 to be injected in WAG. This generates CO_2-in-brine foam in the reservoir (Xing et al., 2010).

In designing WAG injection, slug size, amount HCPV injected during each cycle, WAG ratios are some of the design parameters that are optimized for efficient implementation (Chen et al., 2010; Guo et al., 2006; Shedid et al., 2008). Unstable

pressure distribution, early gas break-through and low oil recovery are challenges that may result due improper selection of the aforementioned parameters (Chen et al., 2010). The optimum CO_2 slug size during WAG injection has been reported in the literature to be 15% HCPV injected (Ghomian et al., 2008; Guo et al., 2006; Shedid, 2009). Smaller WAG injection ratios have higher oil recoveries but lead to early break-through as the ratio becomes smaller (Guo et al., 2006). WAG ratio of 0.6 (Ghomian et al., 2008) and $1:1$ Guo et al. (2006) have also been reported in the literature.

2.3.3 Other CO_2 Injection Methods

One of the major problems of CO_2 flooding is lack of mobility control. This problem has seen different solutions being investigated. Other modes of CO_2 injection have been studied and have been applied in the field. Among these methods, Surfactant Alternating Gas (SAG) and Foam Assisted Water Alternating Gas (FAWAG) use surfactant to control the mobility of CO_2 (Ren et al., 2011). SAG injection has an advantage over continuous foam injection to control mobility of CO_2 (Kloet et al., 2009). In both methods, surfactant is dissolved in either water (SAG,FAWAG) or gas (FAWAG). When the surfactant is dissolved in gas it is also referred as Water Alternating Gas with dissolved Surfactant (WAGS). In this study WAGS is used interchangeably with FAWAG. World largest field application of FAWAG is in Snorre field (Spirov et al., 2012).

2.4 Application of Surfactant in CO_2 Flooding

Surfactant is used to reduce the mobility of CO_2 by increasing its viscosity. Reducing the mobility of CO_2 leads to higher sweep efficiency. Also, capillary forces between oil and water are reduced due to reduction in interfacial tension by the surfactant (Andrianov et al., 2011). The amount of surfactant for foam generation and propagation in CO_2 foam flooding strongly affects the economics of the flooding (Fjelde et al., 2008). For successful implementation CO_2 foam, the surfactant used in foam generation should have the following attributes; efficient at MMP, non-ionic, non-fluorous, CO_2-philic hydrocarbon tails, ethylene oxide hydrophiles and water soluble (Xing et al., 2010).

Chaser international CD 1045 anionic surfactant have also been used in many investigations. This anionic surfactant has been found to be effective on carbonate rocks (Fjelde et al., 2009). Alpha olefin Sulfonate (Farajzadeh et al., 2009) and DOW chemicals surfactants (LE et al., 2008) have also been applied in the field and core floods. Adsorption of surfactants onto rock surfaces is due to their amphipatic nature (Tsau and Heller, 1992). Main factors affecting the adsorption of surfactant onto rock surface are; surfactant nature, temperature, salinity and hardness, rock type, wettability and presence of residual oil (Khalil and Asghari 2006). The presence of residual oil presence increased the adsorption of $CD1045$ by about 32% (Moradi-Araghi, Johnston et al. 1997). To satisfied the requirement for permanent adsorption, additional amount of surfactants are needed for CO_2-foam propagation (Tsau and Heller, 1992). Co-surfactants system has been

suggested as a means of reducing the amount of expensive surfactants (Grigg et al., 2002). Adsorption of surfactants contributes 90% consumption of surfactants in the reservoir and partitioning into crude oil consumes about 30% (Grigg and Mikhalin, 2007; Grigg et al., 2002). To improve the utilization factor and hence reduce cost requires proper formulation of the surfactants that are tolerant to adsorption and partitioning (Bian et al., 2012).

2.5 Foam Application in CO_2 Flooding

Foam consists of surfactant, water and gas (Kloet et al., 2009). Foam is a medium by which CO_2 breakthrough is delayed to result in a favorable oil recovery (Syahputra et al., 2000). Thin pore-spanning liquid films separate the gas bubbles (Kloet et al., 2009). Foam is formed in-situ in the reservoir when injected gas and injected water with dissolved surfactant come into contact or formed at the surface before injection (Shi and Rossen, 1998). Foam duty essentially is to reduce the gas mobility (i.e. CO_2) thereby increasing sweep efficiency and delay of CO_2 breakthrough (Zuta and Fjelde, 2011). Foam generated in-situ occur in high permeability zones first which causes more fluids to flow to low permeability zones (Skoreyko et al., 2012). The generated foam from a given surfactant is dependent on time, oil saturation and capillary pressure (Skoreyko et al., 2012). Foam injected into the reservoir can separate into gas and liquid phases due to gravity segregation (Shi and Rossen, 1998; Zuta and Fjelde, 2011).

The surfactant dissolved in water transport in the matrix contributes to reduction of IFT between oil and water causing changes in wettability and residual oil saturation reduction (Skoreyko et al., 2012, 2011). Economics of foam flooding is highly dependent on the quantity of surfactant used in generation and propagation (Grigg et al., 2002). Improved economics due to efficient sweep, decrease in the cost additives, improved injectivity and/or decreased gas production make foam CO_2-foam flooding attractive (Grigg et al., 2002). To evaluate the efficiency of foam flooding, a Mobility Reduction Factor (MRF) defined in Eq. 2.1 is used (Bian et al., 2012).

$$MRF = \frac{(\Delta P/L)_{foam}}{(\Delta P/L)_{gas}} \tag{2.1}$$

High MRF means more pressure drop, which means gas mobility reduction by the foam. MRF is determined in the laboratory by first co-injecting gas and brine until pressure drop across the core stabilizes. Surfactant and gas are then co-injected until pressure drop is steady, then surfactant, gas and oil are co-injected until the pressure drop in the core is steady.

The strength of foam measured in laboratory coreflood may not correspond to its strength at the field scale (Kloet et al., 2009). Foam application in laboratory and numerical simulation (Zuta, Fjelde and Berenblyum, 2010) and field trials (Blaker et al., 1999; Spirov et al., 2012) have proven to be successful in improving oil recovery. CO_2 foam experiments have been shown experimentally to recover $3-5$ time incremental recovery after waterflooding when compared to CGI and WAG in fractured chalks (Zuta, Fjelde, Berenblyum, Vartdal and Ovesen, 2010).

Foam quality, water saturation and injection strategy are factors that affect oil recovery during foam flooding (Zuta and Fjelde, 2011). The strength of foam is increased with increasing foam quality (Chang and Grigg, 1998). When foam is exposed to oil, high reservoir temperature and high formation salinity, the efficiency of the foam decreases (Bian et al., 2012; Spirov et al., 2012). Adsorption of surfactant onto rock surfaces also decreases its efficiency. In matching the performance of laboratory foam performance to field performance, mobility control as function of foam quality is very important and hence correct foam density must be calculated (Skoreyko et al., 2012). Empirical and mechanistic models are the two main methods in numerical simulators for modeling foam (Skoreyko et al., 2012). Mechanistic modeling of CO_2-foam flooding, requires that we have reliable information on foam quality, foam density, foam degradation, foam regeneration, mobility control, water-oil IFT reduction, surfactant adsorption and non-Newtonian flow (Skoreyko et al., 2012).

2.6 CO_2 Flooding Optimization

In optimizing CO_2 flooding, the following economic factors must be considered; ultimate CO_2 slug size, injection strategy (CGI, WAG, FAWAG, SAG), effect of the operating pressure, effect of GOR and GOR controls, infill wells and processing rate (Guo et al., 2006). The objective function usually maximized in CO_2 flooding for EOR purpose is NPV (Chen et al., 2010). To maximize the objective function, design variables generated by the optimizer are written in the simulator input file

at each iteration level. The design variables for CO_2 flooding are injection rates, ratio of gas slug size to water slug size, cycle time for each injected fluid, mobility ratio between water and oil, location of gas and water injectors and the BHP of producers (Chen et al., 2010; Mirkalaei et al., 2011). Utilization factor (UF) is the industry means of measuring the performance of CO_2 flooding in the field. UF is defined mathematically as;

$$UF_{CO2} = \frac{V_{CO2}(MSCF)}{Q_o(bbl)} \tag{2.2}$$

UF of $5 to 10 Mscf/bbl.$ is the accepted industrial range (Zhou et al., 2012). UF is defined as the volume of CO_2 injected at standard conditions to produce a barrel of oil (Kulkarni and Rao, 2005).

GA is the popular optimization algorithm in the petroleum industry (Harding et al., 1998) but the technique is computationally expensive when applied to field scale optimization (Chen et al., 2010). In the petroleum industry, new optimization algorithms are gradually replacing the GA as an optimizer. Example of such algorithms are differential evolution (Jahangiri and Zhang, 2011), particle swarm optimization (Onwunalu and Durlofsky, 2010) and adjoint based optimization which require access to simulator code (Odi et al., 2010). To the best of our understanding, two non-adjoint based algorithms have been applied in optimizing CO_2 flooding. They are GA (Chen et al., 2010) and DE. In this study, CMA-ES and DE were used in optimizing CO_2 foam flooding.

CHAPTER 3

OPTIMIZATION ALGORITHMS AND FOAM MODEL

3.1 Optimization Algorithms

Several stochastic optimization algorithms have been implemented to solve petroleum problems. In this work, CMA-ES and DE are chosen as the optimization algorithms for optimizing NPV in CO_2 foam flooding process. These two algorithms are all derivative free algorithms. The algorithms generate solutions stochastically and do not need access to simulator codes. Description of how each of these algorithms works is explained in subsequent subsections. Other performance parameters that were used in analysis for the optimized foam flooding evaluations are; field pressure response, and field recovery efficiency.

3.1.1 Covariance Matrix Adaptation-Evolutionary Strategy

CMA-ES is an evolutionary algorithm that mimics biological process of mutation, recombination and selection. CMA-ES search for optimal solution by adapting the covariance matrix and mean of selected offspring generated from a normal distribution in each iteration level to move towards the global solution. In CMA-ES optimization algorithm, population points (λ) are sampled from a multivariate normal distribution at each iteration run (Hansen and Ostermeier, 2001; Bouzarkouna et al., 2011). At each iteration (t), m represents the mean of solutions generated at the current iteration for the optimum solutions. σ and C are step size and covariance matrix respectively. Multivariate normal distribution search points $x_1^{t+1}, x_2^{t+1}, ..., x_\lambda^{t+1}$ m^t,C^t and σ^t are generated for each iteration as in Eq 3.1;

$$x_i^{t+1} = m^t + \sigma^t y_i(0, C^t), \forall i = 1, ..., \lambda \tag{3.1}$$

To move to the next iteration $t+1$ the best solutions (μ) selected based on the evaluated objective function in this case the NPV. m^{t+1}, C^{t+1} and σ^{t+1} is updated from the selected best solutions. The weighted mean m^{t+1} is updated base on the formula (Eq 3.2);

$$m^{t+1} = \sum_{i=1}^{\mu} \omega_i x_{i:\lambda}^{t+1} \tag{3.2}$$

where ω_i, for $i = 1, ..., \mu$ is the weighting coefficients (Eq 3.3)

$$\sum_{i=1}^{\mu} \omega_i = 1, \omega_1 \geq \omega_2 \geq ... \geq \omega_\mu > 0 \tag{3.3}$$

To calculate the step-size to move to the next iteration, the mean trajectory is calculated as in Eq 3.4 which is updated using Eq 3.5

$$p_\sigma \leftarrow (1 - c_\sigma) p_c + \sqrt{c_\sigma (2 - c_\sigma) \mu_{eff}} C^{-\frac{1}{2}} \frac{m^{t+1} - m^t}{\sigma^t} \tag{3.4}$$

$$\sigma \leftarrow \sigma \times \exp \left[\frac{c_\sigma}{d_\sigma} \left(\frac{\|p_\sigma\|}{E \|\aleph (0, I)\|} - 1 \right) \right] \tag{3.5}$$

Once the step-size is updated, the weighted covariance matrix from from the sampled population is adapted using Eq 3.6

$$C^{t+1} = (1 - c_1 - c_\mu) C^t + c_1 p_c^{t+1} p_c^{(t+1)^T} + c_\mu \sum_{i=1}^{\mu} \omega_i y_{i:\lambda}^{t+1} \left(y_{i:\lambda}^{t+1} \right)^T \tag{3.6}$$

p_c in Eq 3.6 is calculated using Eq Eq 3.7

$$p_c \leftarrow (1 - c_c) p_c + h_\sigma \sqrt{c_c (2 - c_c) \mu_{eff}} \frac{m^{t+1} - m^t}{\sigma^t} \tag{3.7}$$

Where

$$c_1 \approx 2/n^2$$

$$c_\mu \approx \min (\mu_{eff}/n^2, 1 - c_1) \, and$$

$$y_{i:\lambda}^{t+1} = \left(x_{i:\lambda}^{t+1} - m^t \right) / \sigma^t$$

The solutions are ranked according the objective function (Equation 3.8) evaluation and the best points are selected to the next iteration. The same process is repeated until the stopping criterion is met.

$$f(x_{1:\lambda}) \leq f(x_{\mu:\lambda}) \leq f(x_{\lambda:\lambda}) \tag{3.8}$$

3.1.2 Differential Evolution

In 1996, DE was first introduced (Storn and Price, 1996). DE minimizes the objective function iteratively based on a given quality of solutions (Storn, 1996). DE is a member of derivative free evolutionary optimization algorithms. DE has been implemented in petroleum industry for optimizing CO_2 sequestration (Jahangiri and Zhang, 2011) and for automated history matching (Hajizadeh et al., 2010). These evolutionary algorithms use algebraic equations to mimic biological mutation, recombination and selection process to optimize an objective function. These three biological processes occur at each generation (iteration, t). To optimize the objective function in this study (i.e. NPV), we select some design variables (D) for this study time for water injection half cycle and well locations. We select the size of the population ($\aleph$) which cannot be less than 4 to search for the optimal solution where the choice of $\aleph$ is;

$$\aleph = 4 + floor[3 \times \log(\text{dim})] \tag{3.9}$$

Where dim is the dimension of the problem. This form represents the design variable vector.

$$X_{1,t} = [X_{1,i,t}, X_{2,i,t}.....X_{D,i,t}]\, i = 1, 2, ..., \aleph \tag{3.10}$$

The upper and lower boundary for each design variable is defined as $X_j^L \leq X_{j,i,1} \leq X_j^U$ which is randomly selected uniformly from $\left[X_j^L, X_j^U\right]$.

First selecting randomly three distinct vectors mutate each design variable vector $X_{i,t}$. Let say we select $X_{r1,t}, X_{r2,t}, X_{r3,t}$, the weighted difference of two of the vectors is added to the third vector as in the Eq 3.11

$$V_{i,t+1} = X_{r1,t} + F(X_{r2,t} - X_{r3,t}) \tag{3.11}$$

F is constant $[0, 2]$ and $V_{i,t+1}$ is the mutated vector.

A trial vector $U_{i,t+1}$ is formed by mixing the mutated vector $V_{i,t+1}$ and target vector $X_{i,t}$. The trial vector is given by

$$\begin{aligned} &U_{i,t+1} = (U_{1i,t+1}, U_{2i,t+1}, ..., U_{Di,t+1}) \\ &where \\ &U_{ji,t+1} = \left\{ \begin{array}{l} V_{ji,t+1}, if \mathrm{rand\,(j, i)} \leq CR \mathrm{orj = rand(i)} \\ \mathrm{X_{ji,t}}, if \mathrm{rand(j, i)} > CR \mathrm{randj \neq rand(i)} \end{array} \right\} \end{aligned} \tag{3.12}$$

$i = 1, 2, ..., N$ and $j = 1, 2, ..., D$

$rand(j, i) \sim U\,[0, 1]$ and $rand(i)$ is generated randomly from $[1, 2, ..., D]$ so that

$V_{i,t+1} \neq X_{i,t}$. $CR \in [0,1]$ the user determines this.

The target vector $X_{i,t}$ is compared with the trial vector $U_{i,t+1}$. Since it is a minimization problem, the vector with the lowest objective functional value is selected for the next iteration else, the old value is retained for the next iteration.

$$X_{i,t+1} = \begin{cases} U_{i,t+1} iff(U_{i,t+1}) \leq f(X_{i,t}) \\ X_{i,t} otherwise \end{cases} \quad i = 1, 2, ..., N \tag{3.13}$$

3.2 Objective Function

The objective in this work is to optimize the NPV in CO_2 foam flooding. For the first case, it was assumed the reservoir has already undergone waterflooding and CO_2 foam flooding is to be implemented. The second case involves the study of well placement using these algorithms to optimize NPV. After the optimum well locations are determined, we optimize the duration of water injection half cycle with NPV as our main objective function. NPV is a commonly used performance measure for management of petroleum reservoir exploitation. NPV equation used by (Bender, 2011) was modified to form the new NPV for CO_2 foam flooding. The equation for NPV used as the objective function is

$$NPV = \sum_{n=1}^{N} \frac{\text{oilRevenue}_n - \text{recurrentCost}_n}{(1+r)^n} - Capex \tag{3.14}$$

N is the total number of years of production, r is the annual discount rate; oilRevenue_n is the total revenue from oil production at each year and Capex is

the cost of surface facility installation and well drilling cost. recurrentCost$_n$ is the total cost due to water production, water injection, CO_2 injection and surfactant injection. Where recurrentCost$_n$ is given by

$$\begin{aligned}\text{recurrentCost} = \text{gasPurchase} + \text{recyclingCost} + \text{watInjCost} \\ + \text{gasInjCost} + \text{liftCost} + \text{surfInjCost}\end{aligned} \quad (3.15)$$

$$gasPurchase = [Q_{gi}(n) - Q_{gi}(n-1)] - [Q_{gp}(n) - Q_{gp}(n-1)] \times \text{gasPrice} \quad (3.16)$$

In Equation 3.16, Q_{gi} is the total gas injected at n^{th}, Q_{gp} is the total gas produce at n_{th} and gasPrice is the price of gas purchased ($USD/MSCF$). This determines the cost of gas purchased out of the total amount of gas injected.

$$\begin{aligned}recyclingCost = [Q_{gp}(n) - Q_{gp}(n-1)] \times \text{gasRecPrice} \\ + [Q_{wp}(n) - Q_{wp}(n-1)] \times \text{watRecPrice}\end{aligned} \quad (3.17)$$

To minimize the amount of injected fluid purchased, the produced injected fluids are recycled. Equation 3.17 defines the cost of recycling produced water and gas. Q_{gp} is the total gas produce at n_{th} and gasPrice is the price of gas purchased ($USD/MSCF$). gasRecPrice is the price of recycling produced gas ($USD/MSCF$) and watRecPrice is the price of recycling water produced (USD/STB).

$$watInjCost = [Q_{wi}(n) - Q_{wi}(n-1)] \times \text{watInjPrice} \quad (3.18)$$

watInjCost in Eq 3.18 is the total cost of injected water less the cost of recycled or is the cost of water needed top up the recycled water for make up the amount of water injected at each year. Q_{wi} is the total water injected at n^{th} year.

$$liftCost = [(Q_{op}(n) - Q_{op}(n-1)] + [Q_{wp}(n) - Q_{wp}(n-1)] \times \text{liftPrice} \quad (3.19)$$

liftCost is the operational cost of transporting of produced oil and production operations. Q_{op} is the total oil produce at n_{th} year and liftPrice is the price per STB of oil and water produced handling.

$$surfInjCost = [Q_{si}(n) - Q_{si}(n-1)] \times \text{surfPrice} \quad (3.20)$$

surfInjCost is the total cost of injecting surfactant at each year. Q_{si} is the total surfactant injected at n_{th} year and surfPrice is the price of surfactant injected per *lb*.

3.3 Design Parameters

The key design parameters for foam flooding optimization process are; surfactant amount,cycle ratio, cycle length injection cycle length, injection-production rates and well locations. In this study, well location and injection ratio between water and gas with dissolved surfactant were used as the controlling variables for the optimization algorithms to optimize NPV. The other design parameters (i.e. injection rates, cycle length and surfactant amount) were determined from sensitivity studies.

3.3.1 Well Locations

Determining the proper locations of wells in reservoir exploitation is key to efficient displacement. We optimize NPV by determining the proper locations for injection and production wells for a newly discovered field to be developed. To optimize these locations Schlumberger ECLIPSE-100 and MATLAB are integrated for the optimization process. Schlumberger ECLIPSE-100 simulator serves as objective function evaluator. CMA-ES and DE, written in MATLAB, serve as objective function optimizers for the control variables and change the well locations. These new locations are evaluated to determine the NPV. The same process is repeated until stopping criteria are met, and then we take those locations as the optimum locations for the field.

3.3.2 Cycle Ratio

One important design parameter during water alternating gas injection process is the ratio between the gas injection period and the water injection period. The cycle length is the sum of water injection periods (water half cycle) and the gas injection periods (gas half cycle). This ratio determines how effective the displacement process can be. The number of cycles for duration of the prediction and the cycle length were determined from sensitivity test and the cycle ratio was optimized using the optimizing algorithms. In the optimization process, the duration of water injection half cycle was changed between 1 day to 700 days and the remaining days for gas injection half cycle for each cycle length. The total number of days for each cycle length is 731.

3.4 Foam Flood Modelling In ECLIPSE

Schlumberger ECLIPSE 100-simulator models foam as a tracer which is transported in water or gas phase (Schlumberger, 2010). The modeling takes into account the adsorption of foam onto rock surfaces and the decay of foam with time. In foam flooding essentially, what the foam does is to reduce the mobility of the injected gas. The simulator does not model the detail physics of foam flooding. In Schlumberger ECLIPSE 100, the foam is modeled as effective concentration of surfactant existing in gas or water phase, which exist in the form of foam. Schlumberger ECLIPSE 100 models foam in gas phase using the following

conservation equation (Schlumberger, 2010);

$$\frac{d}{dt}\left(\frac{V_s S_g C_f}{B_r B_g}\right) + \frac{d}{dt}\left(V\rho_r C_f^a \frac{1-\phi}{\phi}\right) = \sum\left[\frac{Tk_{rg}}{B_g\mu_g} M_{rf}\left(\delta P_g - \rho_g g D_z\right)\right] C_f + Q_g C_f - \lambda\left(S_w, S_o\right) V C_f \quad (3.21)$$

Where

ρ_g = density of gas

C_f^a = foam concentration

μ_g = viscosity of gas

B_r = rock formation volume

B_g = gas formation volume factor

T = transmibility

k_{rg} = gas relative permeability

S_g = gas saturation

V = block pore volume

Q_g = gas production

P_g = gas pressure

M_{rf} = mobility reduction factor

Adsorption term in Eq 3.21 is modeled with the assumption that adsorption to occur instantaneously and is defined by the term $V\left(\frac{1-\phi}{\phi}\right)\rho_r C_f^a$. ECLIPSE 100 provides two options for adsorption data, either a table of foam adsorbed as a function of foam concentration is supplied or an analytical adsorption model using the Langmuir isotherm is used. In this study, we used the first option using sample adsorption data file in ECLIPSE 100. The foam adsorption term is optional in Schlumberger ECLIPSE 100 but, we enabled that option. The decay of foam is modeled by the term $\lambda\left(S_w, S_o\right)$ which is a function of both water and oil saturation. This term also is optional but we enabled this term with both data from ECLIPSE 100 example input file.

The mobility of the injected gas in the reservoir is reduced using the mobility reduction factor (M_{rf}). There are two options in ECLIPSE 100, either the functional form or the tabular form. The functional form is used when foam is declared to be in the water phase. Since we used the foam in the gas phase, the tabular option was used in this study M_{rf} for modeling. The M_{rf} is defined for tabular form in ECLIPSE 100 as in Eq 3.22;

$$M_{rf} = \left(1 - M_{rf}^{cp}\right) M_v\left(V_g\right) + M_{rf}^{cp} \tag{3.22}$$

$$M_{rf}^{cp} = \left[1 - M_c\left(C_f\right]\right) M_p\left(P\right) + M_c\left(C_f\right) \tag{3.23}$$

Where

$M_v(V_g)$ = mobility reduction modifier due to gas velocity

$M_c(C_f)$ = mobility reduction factor due to foam concentration

$M_p(P)$ = mobility reduction modifier due to pressure

P = oil phase pressure

V_g = gas velocity

3.5 Miscible Flood Modelling In ECLIPSE

ECLIPSE 100 models miscibility using Todd-Longstaff empirical model for miscible floods. The model consists of 3-component or 4-component when solvent option is enabled (Schlumberger, 2010). In this study, we used the 3-component model, which consists of reservoir oil, injection gas and water. The injection gas density that was used for this study is that of CO_2 density (Shoaib and Hoffman, 2009). Any reference henceforth to injection gas means CO_2. Todd-Longstaff model modifies the calculation of viscosity and density in black oil simulator. The parameter that ranges between $0-1$ models the effect of physical dispersion in the gridblocks (Todd and Longstaff, 1972). Due to the screening effects of high water saturation Schlumberger ECLIPSE 100 models the effective residual oil saturation that depends on water saturation for miscible flood using Equation 3.24 below (Schlumberger, 2010);

$$S_o^* = MAX(S_o - S_{or}, 0.0) \tag{3.24}$$

Effective gas and oil viscosities and densities and relatives permeabilities for the components in the reservoir for each grid cell are determined using . The option for modeling transition between immiscibility and miscibility was enabled. This option allows for interpolation between PVT properties, relative permeability and capillary pressure calculations during flooding. For the particular table we used data from literature for Arabian medium crude (Oskay et al., 1989).

CHAPTER 4

RESERVOIR SIMULATION MODEL

4.1 Reservoir Description

Two cases were studied in this work. Case 1 involves optimization of foam flooding for 10 years after 21 years of waterflooding for for field which has reach tertiary recovery stage. Case 2 involves a newly discovered field, the optimization involves well placement optimization foam flooding for 10 years after 21 years of waterflooding. The same reservoir model was used for both cases. The reservoir consist of four layers discretized into $50 \times 50 \times 4$ gridblocks. The reservoir model was mainly from Barnawi (2008) and ECLIPSE 100 input files with some from the literature where appropriate for this study. Porosity and permeability for the model was generated using sequential Gaussian simulation. Stanford Geostatiscal Modeling Software (SGEMS) was utilized in generation of permeability values. The

reservoir dimension, porosity and permeability were not the same as in Barnawi (2008). Modification was needed to meet the requirements for this study. Figure 4.1 show the permeability distribution for layers 1 to 4. Table 4.1 gives a summary of the reservoir properties used for this study.

Table 4.1: Reservoir properties.

PARAMETER	**VALUE**
Reservoir dimension (ft)	$13000x13000x120$
Grid dimension	$50x50x4$
Grid block size (ft)	$260x260x30$
Formation depth (ft)	8000
Average horizontal permeability (md)	355.96
Average vertical permeability (md)	35.596
k_v/k_h (md/md)	0.1
Average porosity $(fraction)$	0.181
Rock compressibility (psi^1)	$1.0E^{-9}$
Initial oil saturation $(fraction)$	0.84
Initial water saturation $(fraction)$	0.16

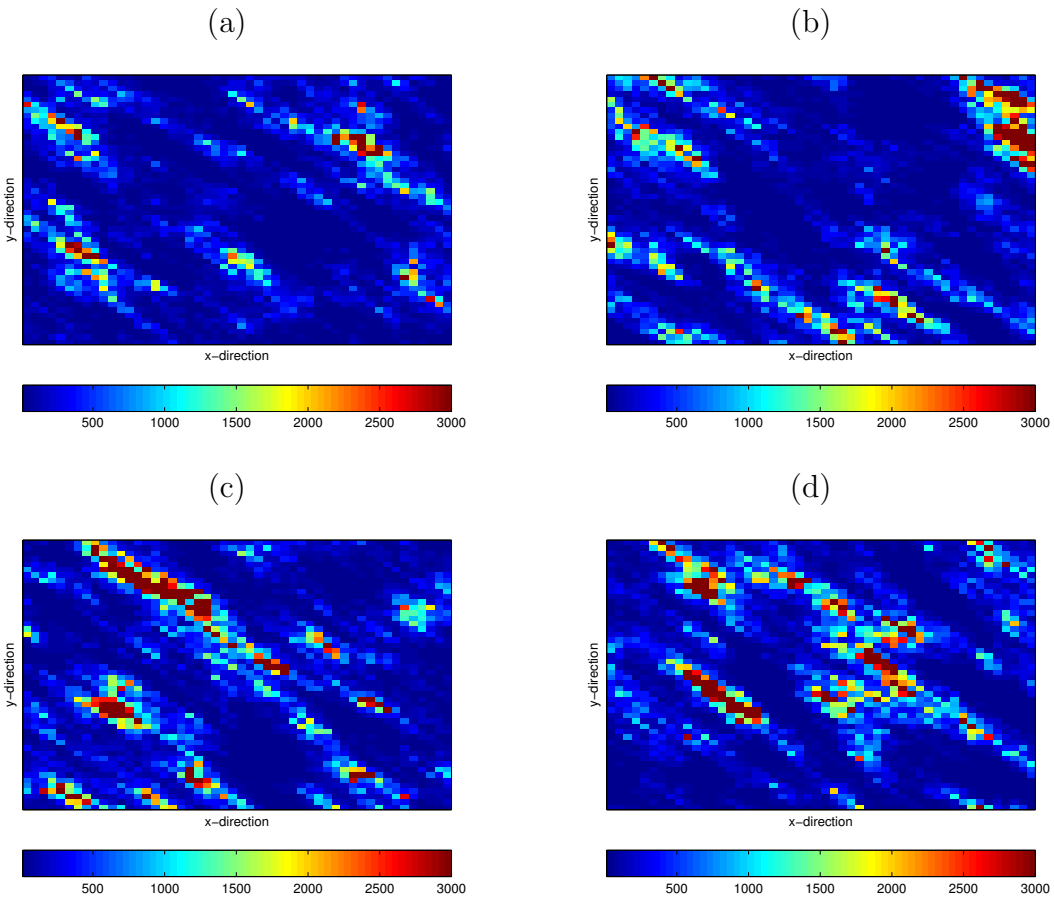

Figure 4.1: Permeability distribution (a) Layer 1 (b) Layer 2 (c) Layer 3 (d) Layer 4

4.2 Reservoir Fluid Description

The PVT properties for oil and gas were taken from Barnawi(2008) as shown in Figs 4.2, 4.3 and 4.4 but the relative permeability dataset was from ECLIPSE 100 sample input data file for the Third SPE Comparative Test data (Fig 4.4). Todd-Longstaff mixing parameter of seven was chosen for miscibility modeling. To model the transition between immiscibility and miscibility, an Arabian medium crude data (Oskay et al., 1989) was used.

Miscibility scale value of zero means the injected gas is immiscible at that pressure while a value of one means injected gas is miscible at that particular pressure. Both TLMX and PMISC keywords are used for modeling miscibility in ECLIPSE 100. TLMX is the required keyword for miscibility runs while PMISC is optional. However in this work, both keywords were enabled since TLMX assumes miscibility occurs at every pressure while PMISC models the transition between immiscible and miscible displacement with respect to pressure. Tables 4.2 and 4.3 show the initial fluid properties and miscibility scale for the simulation model.

Table 4.2: Reservoir fluid properties.

PARAMETER	**VALUE**
Initial pressure ($psia$)	3000
Water compressibility (psi^1)	$1.0E^{-9}$
Water surface gravity	1.07
Water viscosity (cp)	0.31
Water FVF (RB/STB)	1.0
Oil surface gravity (API)	35
Oil viscosity (cp)	0.75
Gas surface gravity	0.7
Gas viscosity (cp)	0.0425

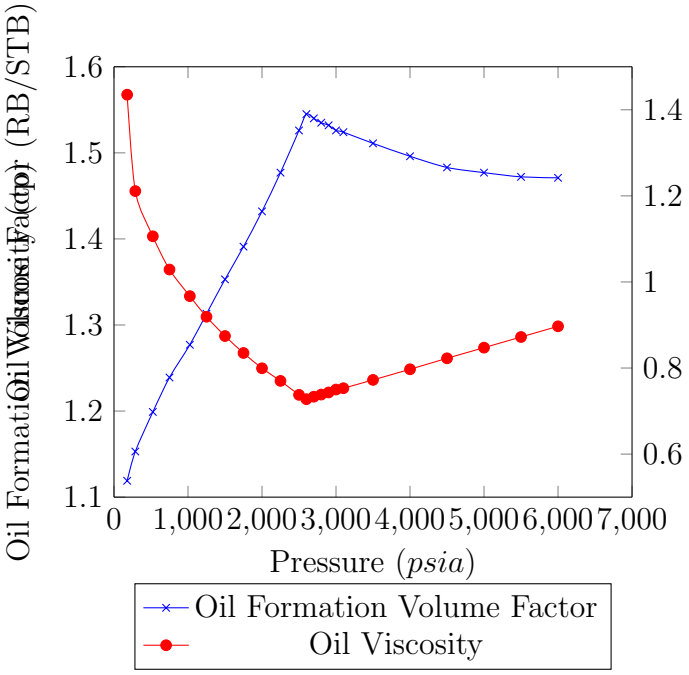

Figure 4.2: Oil formation volume factor and viscosity versus pressure (Barnawi, 2008)

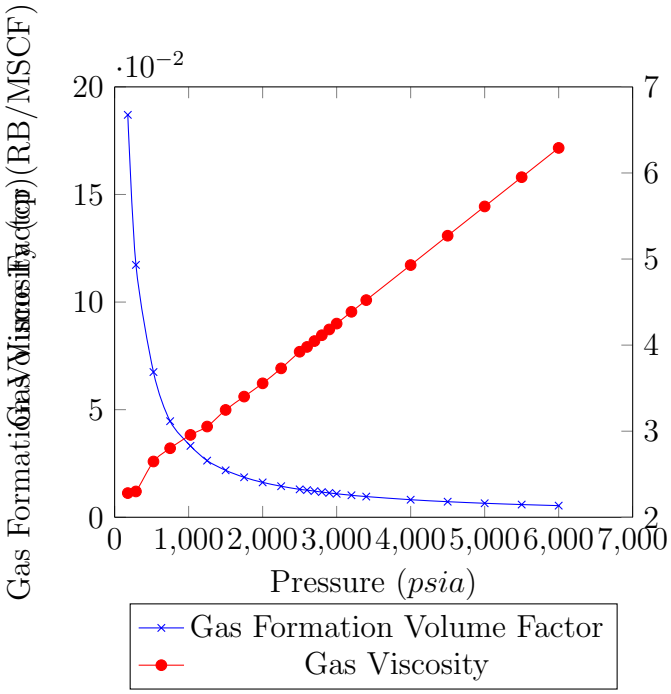

Figure 4.3: Gas formation volume factor and viscosity versus pressure (Barnawi, 2008)

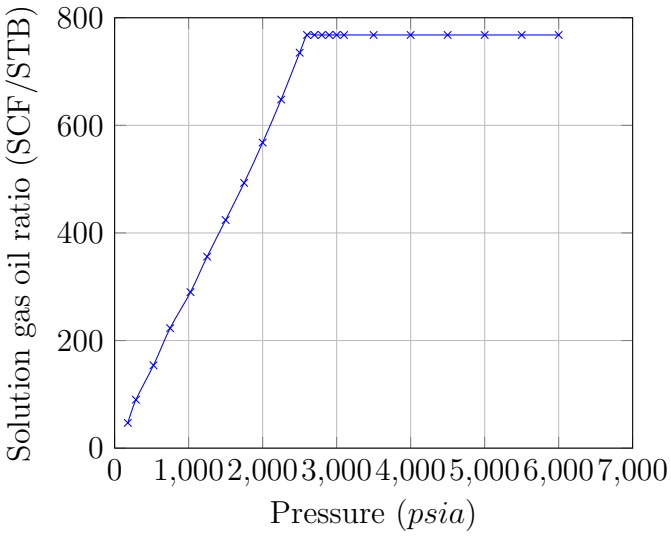

Figure 4.4: Solution gas oil ratio versus pressure (Barnawi, 2008)

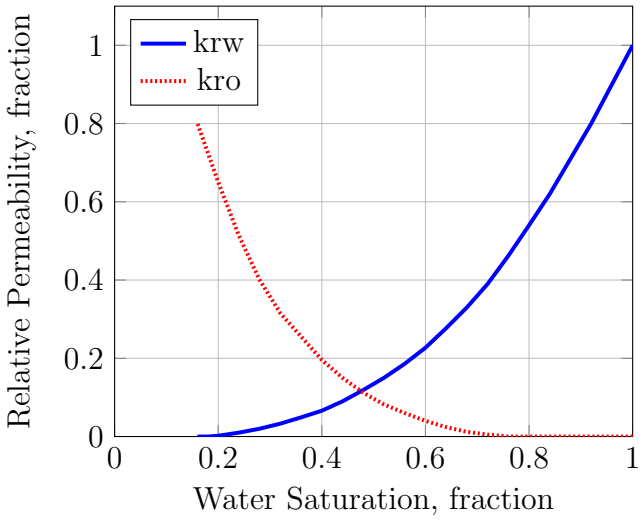

Figure 4.5: Water-oil relative permeability versus saturation

Table 4.3: Miscibility transition.

PRSSURE (*psia*)	**MISCIBILITY SCALE**
2300	0.0 (immiscible)
2400	0.5 (nearly miscible)
3100	1.0 (miscible)

4.3 Foam Properties

Foam properties for both cases were taken from ECLIPSE 100 sample input file for foam in gas. The effects of foam adsorption, foam decay as a function of water and oil saturation, foam mobility reduction, pressure effect on foam mobility reduction and shear rate effect on foam mobility reduction were included in modeling the behavior of foam in the simulation model. Pressure effects on foam data were adjusted to suit the reservoir pressure of the simulation model. Tables 4.4 to 4.7 shows the data for the simulation model.

Table 4.4: Foam Adsorption.

LOCAL FOAM CONCENTRATION (lb/stb)	**ADSORBED CONCENTRATION** (lb/lb)
0	0.00000
1.0	0.00005
30	0.00005

Table 4.5: Foam decay as a function of water saturation.

LOCAL WATER SATURATION	**DECAY HALF-LIFE** ($DAYS$)
0	3000
1.0	2000

Table 4.6: Foam decay as a function of oil saturation.

LOCAL WATER SATURATION	**DECAY HALF-LIFE** ($DAYS$)
0	3000
1.0	2500

Table 4.7: MRF as a function of foam concentration.

FOAM CONCENTRATION	**MRF**
0	1
0.001	0.4
0.1	0.1
1.2	0.05

CHAPTER 5

SENSITIVITY STUDIES

5.1 Sensitivity Studies

Sensitivity studies were conducted before the optimization process to guide in the region to search during the optimization studies or reduce the number of design variables as well as the number of function evaluations. The effects of cycle ratio, cycle length and amount of surfactant injected on the NPV were studied. For cycle length and cycle ratio, water and gas injection rates of 63000 STB/day and 140000 $MSCF/day$ were used respectively and surfactant amount of 1 lb/STB were used for the sensitivity study. The NPV was calculated for 10 years of foam flood. All other properties for the simulation model were the same unless otherwise stated. Table 5.1 shows the field constraints used for both sensitivity and optimization studies and Table 5.2 shows the NPV components. Figure 5.1 shows well locations for sensitivity studies with permeability distribution.

Table 5.1: Field constraints.

CONSTRAINT	VALUE
Total liquid production rate (STB/D)	100000
Total field gas injection rate ($MSCF/D$)	140000
Total water injection rate (STB/D)	63000
Minimum BHP for each producer ($psia$)	2700
Maximum BHP for each injector ($psia$)	4600

Table 5.2: NPV components.

COMPONENT	VALUE
Oil price (USD/STB)	95
Gas purchase price ($USD/MSCF$)	2
Gas recycling cost ($USD/MSCF$)	1
Gas injection cost ($USD/MSCF$)	2
Water injection cost (USD/STB)	3
Water recycling cost (USD/STB)	1
Surfactant cost (USD/LB)	3
Lifting cost of oil (USD/STB)	0.75
Discount rate (annual)	0.1

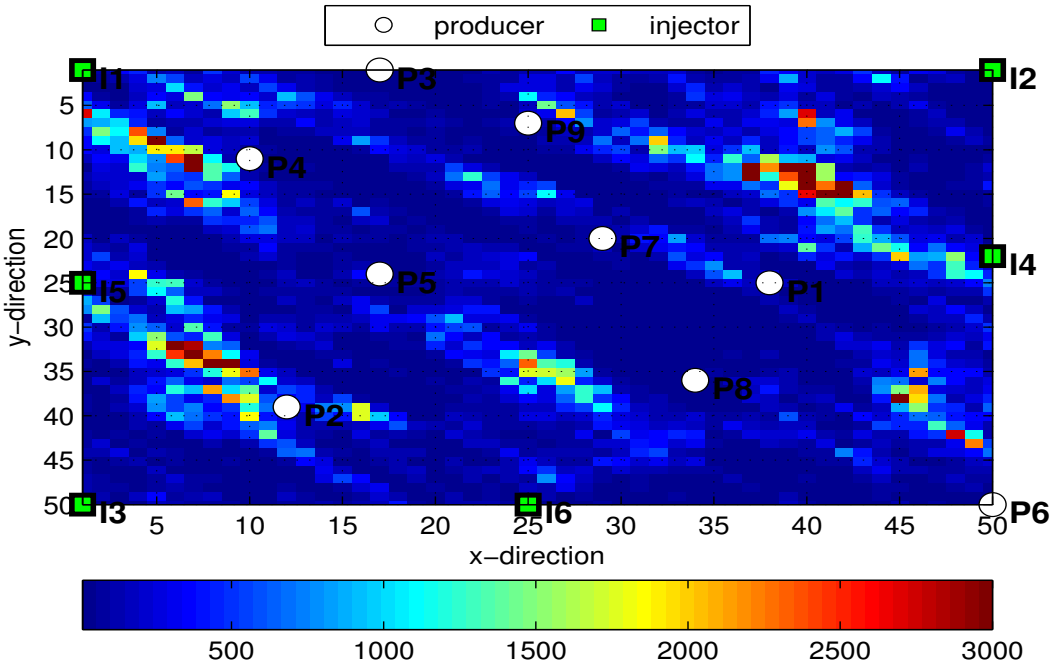

Figure 5.1: Well locations and permeability distribution Layer 1

5.2 Cycle Ratio

Cycle ratio was calculated as ratio of length of time for water injection (t_w) to length of time for gas injection (t_g) at constant injection rate. The maximum BHP for injectors and minimum BHP for producers were also fixed throughout the simulation period. NPV was one of the criteria used in selecting the optimum cycle ratio. Other performance indicators such as field oil recovery efficiency (η_{op}), field oil production rate (Q_{op}) and field pressure (P_f) were also used in the analysis selecting the optimum among the cycle ratios studied. For all three indicators we studied the short term (10 years), medium term (20 years) and the long term (30 years) performance of each ratio for a cycle length of 2 years to determine their effects on the performance of foam flooding.

5.3 Net Present Value

For different cycle lengths, effects of cycle ratios were studied. The ratios were ranked based on NPV for each cycle length for 10 years forward model. The best among them were selected and used for the cycle length comparisons study. It was observed that, a ratio of 0.1 between the water injection period and gas injection period has higher NPV for all cycle lengths as compared to a ratio of two for all cycle lengths for 10 years forward model. This observation can be attributed to the fact that longer gas injection periods lead to more pore volumes injected which leads to increase in average reservoir pressure. The role of gas is to mix with immobile oil and hence making it mobile by reduction of viscosity and density.

The mobile oil is now swept by water. Since the gas is highly compressible the reservoir pressure increases faster thereby achieving miscibility. This also makes more oil mobile and hence with the minimum required amount of water injected efficient sweep is achieved. Lower cycle ratio tends to have more gas injected as compared to higher ratios that is why lower cycle ratio has more recovery as compared with higher ratio. This trend for cycle is similar to what has been reported in the literature for WAG (Guo et al., 2006). Lower cycle ratio of 0.6 has been reported to have higher recovery (Ghomian et al., 2008). All the cycle lengths investigated show increments in field pressure when gas injection started; this resulted in an incremental recovery of oil which resulted in a higher NPV values. The cycle lengths investigated were three months, six months, one year, and two years. Figures 5.2 to 5.5 show the NPV for each cycle length at different ratios.

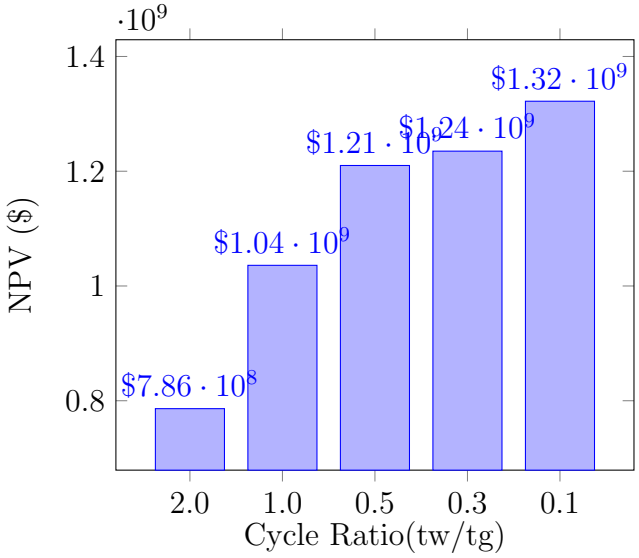

Figure 5.2: NPV for 0.1 to 2.0 for cycle length of 3 months

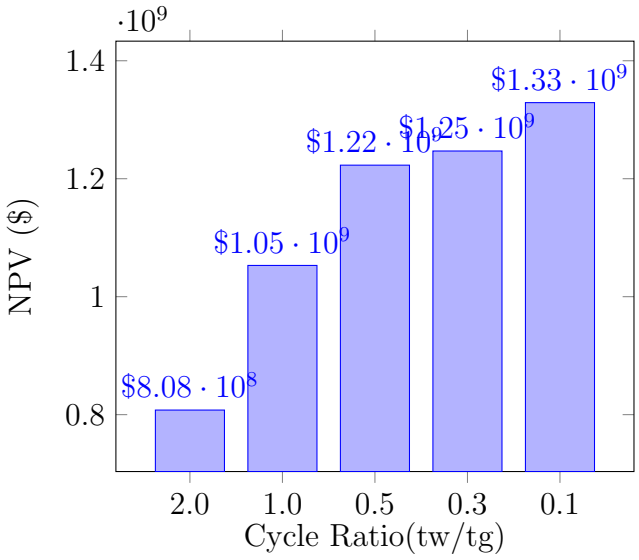

Figure 5.3: NPV for 0.1 to 2.0 for cycle length of 6 months

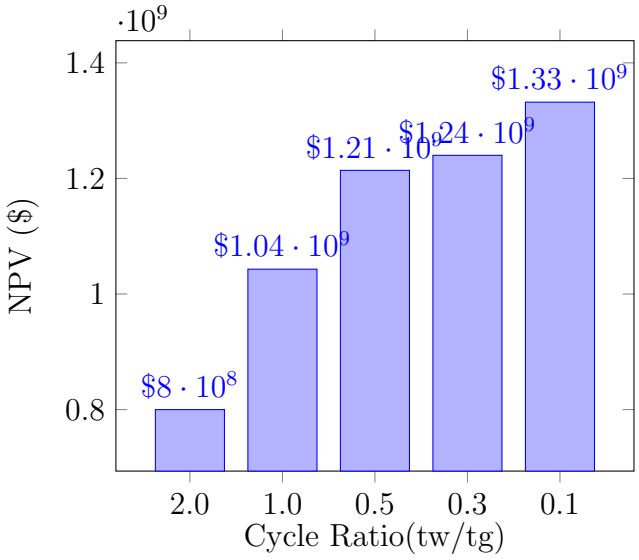

Figure 5.4: NPV for 0.1 to 2.0 for cycle length of 1 year

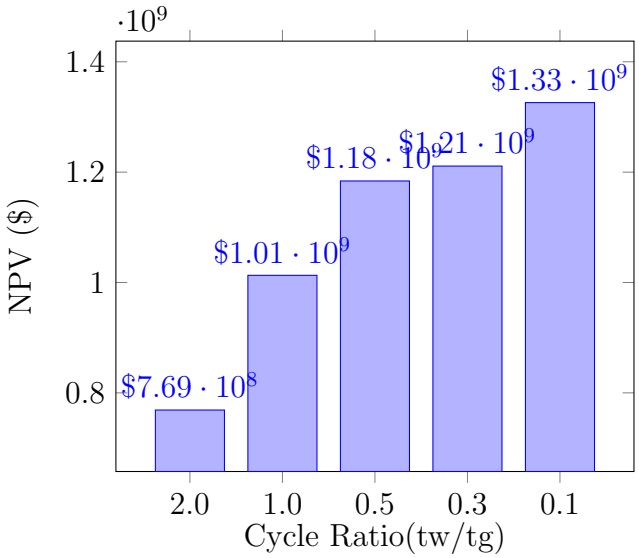

Figure 5.5: NPV for 0.1 to 2.0 for cycle length of 2 years

5.4 Field Oil Production Rate

Comparison for Field Oil Production Rate (Q_{op}) was done for 2 years cycle length to compare the short, medium and long term performance of each ratio. For the short term forward model (Fig 5.6) it was observed that smaller ratios gave higher oil rate than larger ratios. This resulted in higher NPV as noted earlier. The lower ratio had lower performance in the second half (31 to 41 years) of the medium term (Fig 5.7) and all ratios had similar performance in the third half (41 to 51 years) for the long term (Fig 5.8) foam flood.

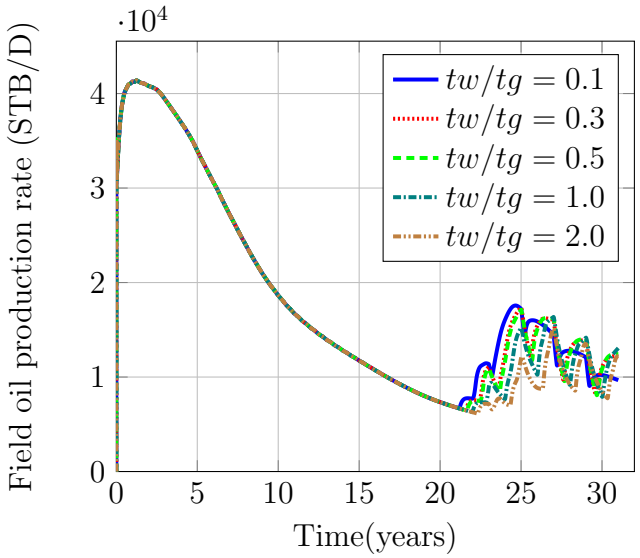

Figure 5.6: FOPR for cycle ratio 0.1 to 2.0 for 10 years foam flood

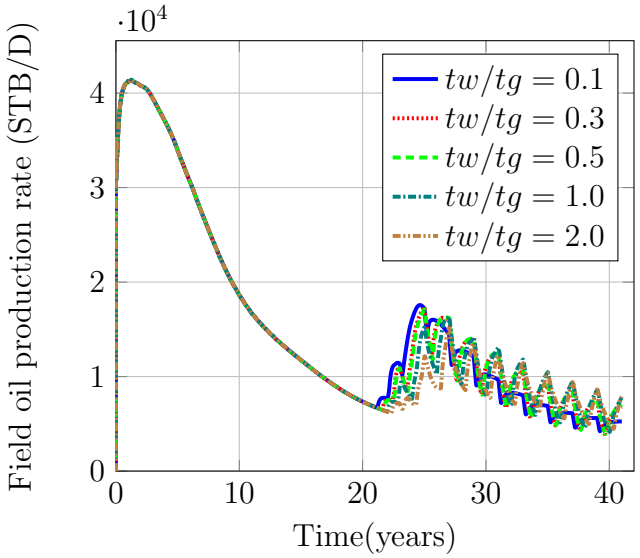

Figure 5.7: FOPR for cycle ratio 0.1 to 2.0 for 20 years foam flood

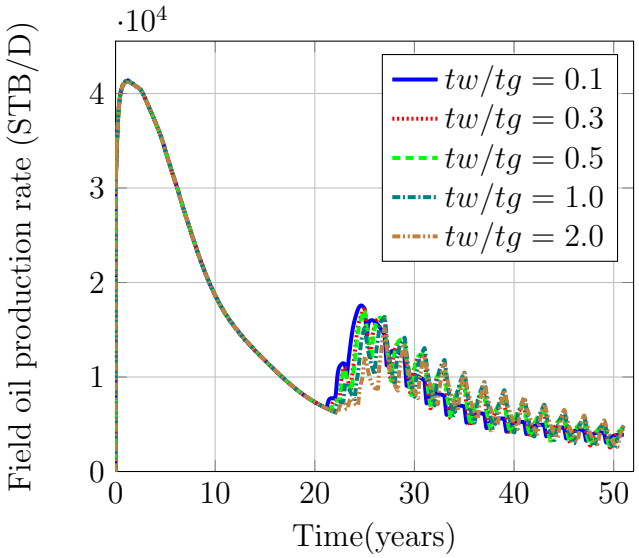

Figure 5.8: FOPR for cycle ratio 0.1 to 2.0 for 30 years foam flood

5.5 Field Pressure and Field Oil Recovery Efficiency

Observation from the Field Pressure (η_{op}) plot (Fig 5.9) shows gentle changes in the pressure for the smaller cycle ratios as compared to larger cycle ratio. The lower cycle ratios had higher Field Oil Recovery Efficiency (P_f) plot (Figure 5.10) due to their injection of higher pore volumes of injection fluids. Also because the smaller cycle ratio injected more gas than water and gas is more compressible than water, the smaller ratios injection resulted in more pore volumes of fluid injected. This resulted in high recoveries. Though higher pressure results in first contact miscibility but may result in reducing the effectiveness of foam (Schlumberger, 2010). Optimum P_f has to be achieved to balance between achieving first contact miscibility and foam effectiveness. This effect of reduction of foam effectiveness at high pressures was captured in the foam modeling that may explain the reasons

why at points where cycle ratio has higher pressure did not result in significant increment in oil recovery. A similar scenario was observed for 20 years (Figs 5.11 to 5.12) and 30 years (Figs 5.13 to 5.14) foam flood.

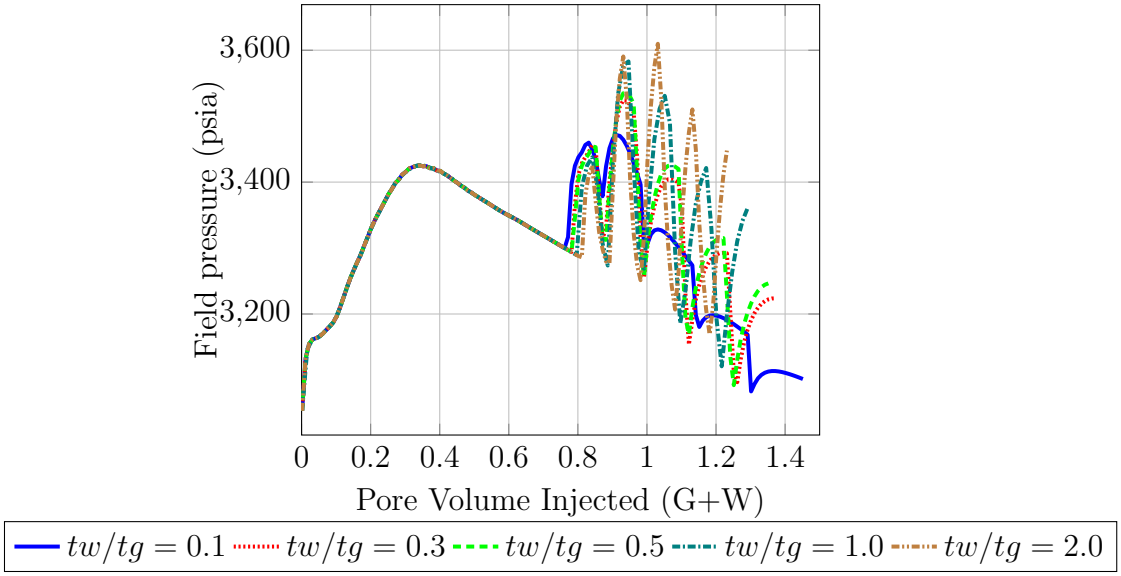

Figure 5.9: FPR for cycle ratio 0.1 to 2.0 for 10 years foam flood

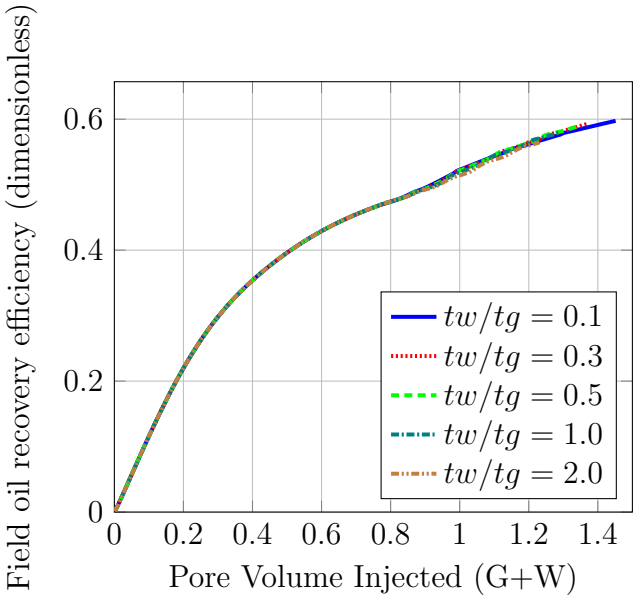

Figure 5.10: FOE for cycle ratio 0.1 to 2.0 for 10 years foam flood

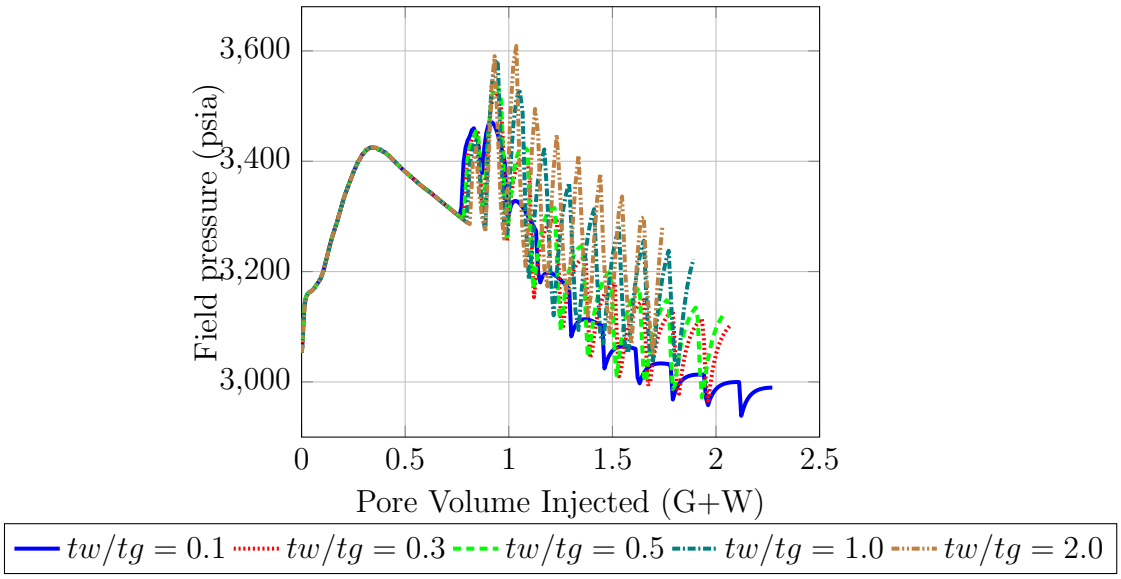

Figure 5.11: FPR for cycle ratio 0.1 to 2.0 for 20 years foam flood

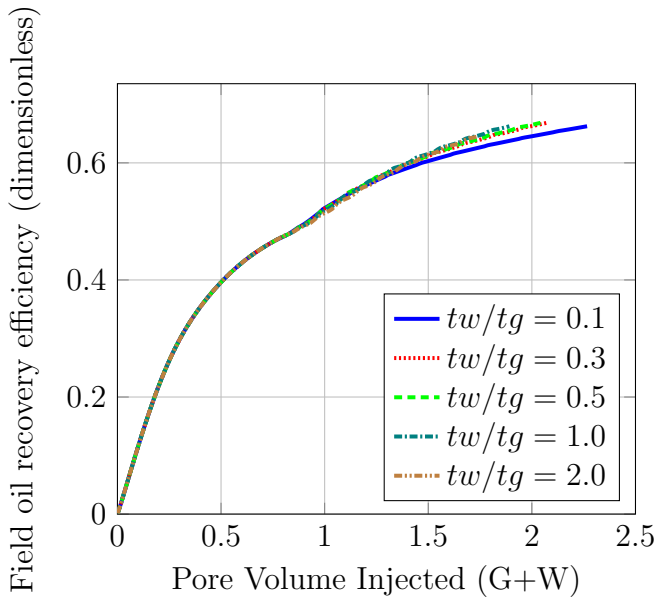

Figure 5.12: FOE for cycle ratio 0.1 to 2.0 for 20 years foam flood

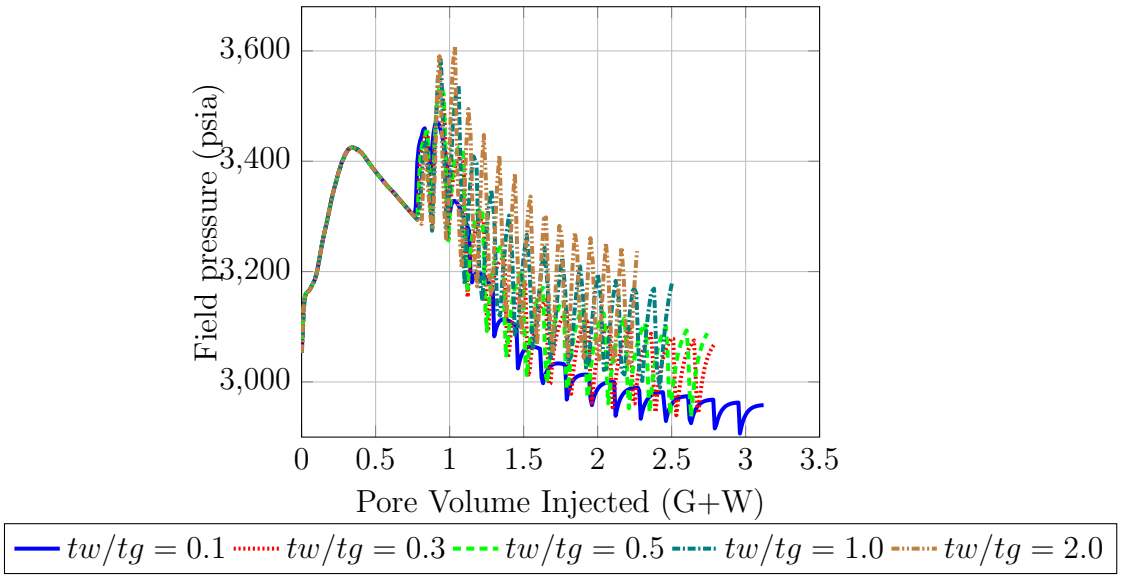

Figure 5.13: FPR for cycle ratio 0.1 to 2.0 for 30 years foam flood

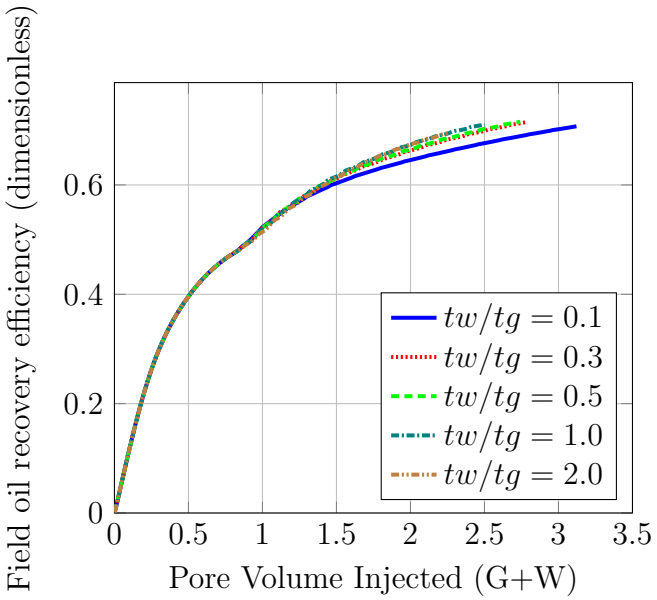

Figure 5.14: FOE for cycle ratio 0.1 to 2.0 for 30 years foam flood

5.6 Cycle Length

Cycle ratio of 0.1 for each cycle length was selected and compared. From the comparisons for cycle ratio, it was observed that longer cycle length had higher NPV. A comparison was then made to determine which cycle length gives the optimum NPV. The comparisons were made for simulation periods of 10 years, 20 years and 30 years to ascertain the impact of cycle length on CO_2 foam flooding. For the durations of foam flood investigated it was observed that there was no significant difference between each cycle length with the same cycle ratio. The two years cycle length was selected for the next sensitivity study of effects of surfactant amount on the NPV. Figure 5.15 shows the NPV for each cycle length studied.

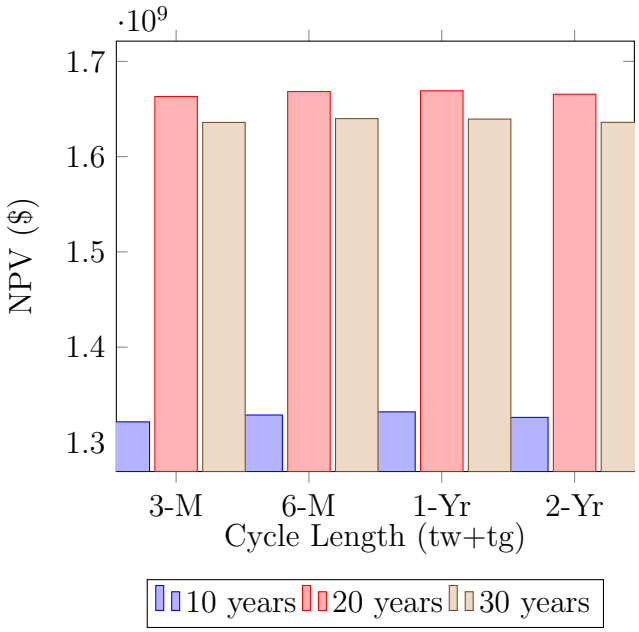

Figure 5.15: Cycle length NPV foam flood for 10, 20 and 30 years.

5.7 Surfactant Amount

Amount of surfactant in foam determines the mobility of the injected foam. The higher the amount of surfactant in the foam, the lower the mobility of the gas in the reservoir. Lower gas mobility in reservoir means less gas produced or more gas stored in the reservoir. Determining the optimum amount of the surfactant that balances between NPV and storage of CO_2 is essential for foam flooding project. In foam flooding, the cost of surfactant cost is a critical component of the recurrent expenditure. Therefore, optimizing the amount of surfactant injected is important. Surfactant amounts of 0.005 lb to 1.2 lb were investigated to determine the amount that gives optimum NPV. In this study, 0.005 lb of surfactant gave the highest NPV due to the fact that this amount does not slow the gas too much. If the objective also is to improve recovery as well as store CO_2

underground, then larger amount of surfactant should be injected. A balance can be achieved between both objectives when WAGS is implemented as compared to WAG method. NPV for foam flooding for 10 and 20 years were investigated. Figures 5.16 and 5.17 shows NPV for surfactant amounts investigated for 10 and 20 years foam flooding respectively. Surfactant amount of 0 lb/stb gave lower NPV as compared with 0.005 lb/stb but gave higher NPV than surfactant amount of 1.2 lb/stb. In terms of the field oil production rate, Figures 5.18 and 5.19 it was observed that surfactant amount of 0.005 lb/stb gave the lowest production rate as compared with higher amounts. Figures 5.20 and 5.21 show the recovery factor for 10 and 20 years foam flooding respectively which follows the same trend as field oil production rate. Though surfactant amount 0.5 lb/stb gave 1.5% and 5% recovery factor for 10 and 20 years foam flooding respectively. The NPV for surfactant amount of 0.005 lb/stb is still higher than surfactant amount 0.5 lb/stb. This can be attributed to the higher cost of surfactant.

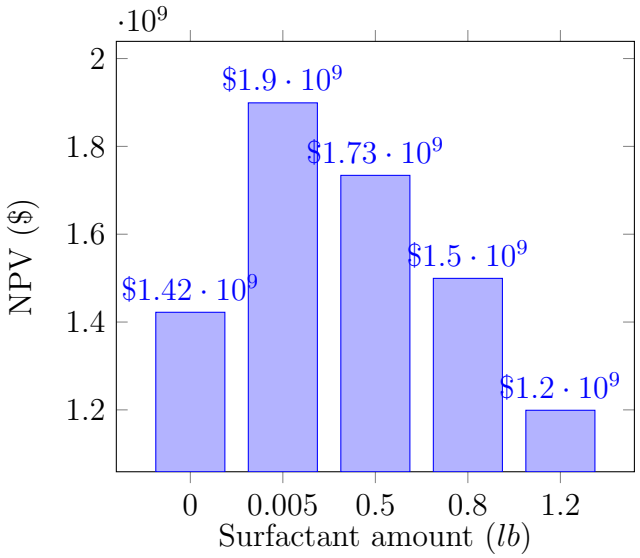

Figure 5.16: NPV for different surfactant amounts (10 years).

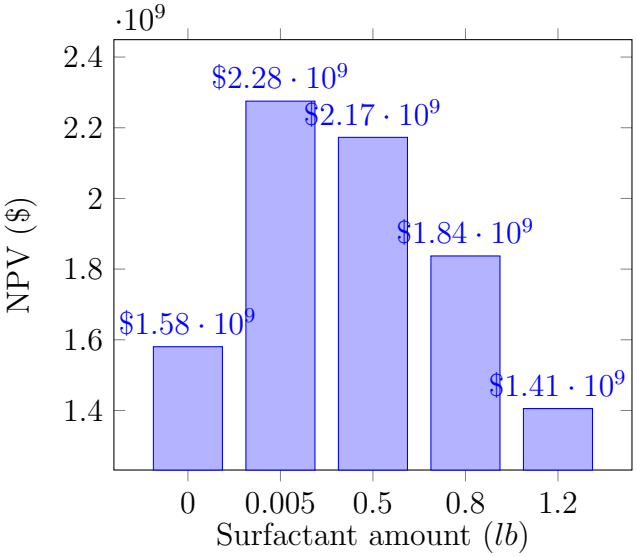

Figure 5.17: NPV for different surfactant amounts (20 years).

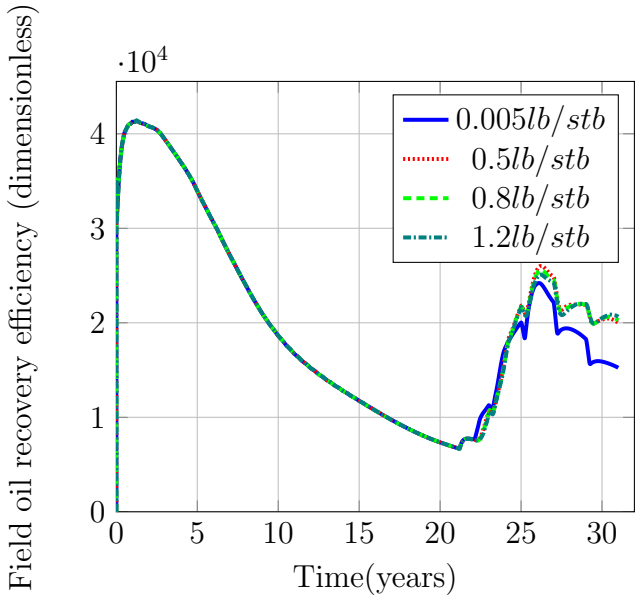

Figure 5.18: Field oil production rate for different surfactant amounts (10 years).

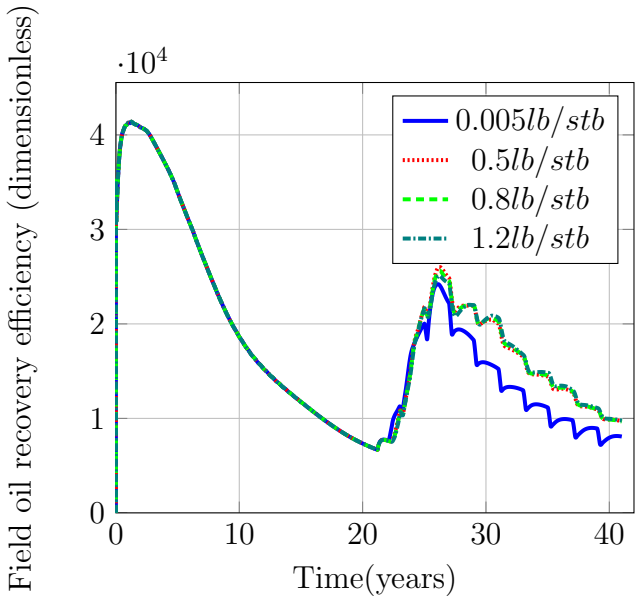

Figure 5.19: Field oil production rate for different surfactant amounts (20 years).

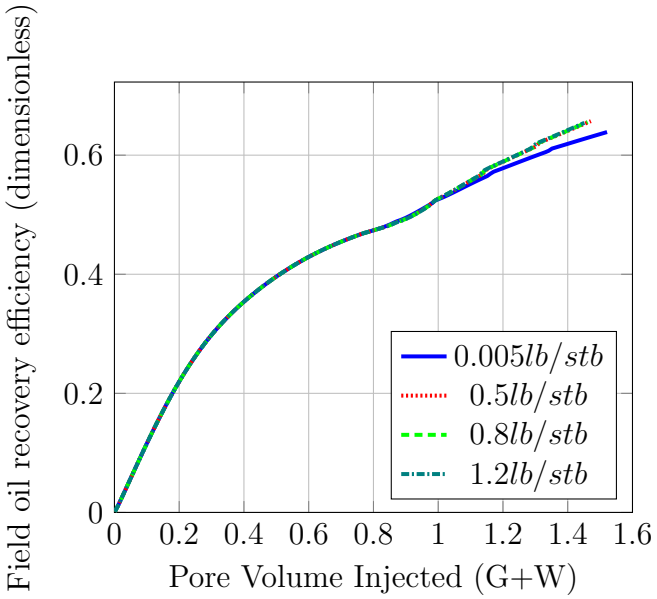

Figure 5.20: Recovery factor for different surfactant amounts (10 years).

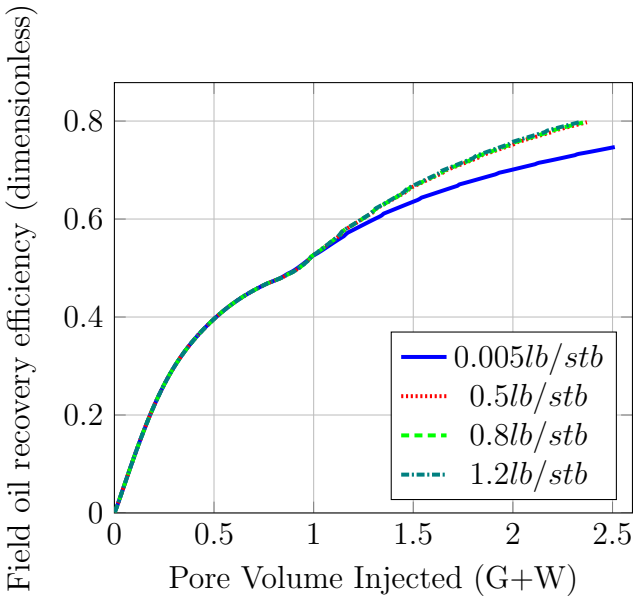

Figure 5.21: Recovery factor for different surfactant amounts (20 years).

5.8 Comparisons of Recovery Methods

Comparison was made for NPV between four different recovery methods. The recovery methods were continuous foam injection (CFI), continuous gas injection (CGI), water-alternating gas (WAG), water-alternating gas with dissolved surfactant (WAGS) and waterflood (WF). The comparisons were made for 10 years, 20 years and 30 years foam flood periods (Fig 5.22). In all flood periods investigated CFI had the highest NPV followed by WAGS, CGI WAG and WATFLD. It was also observed that as the tertiary flood period increases, the NPV's of WAGS and WAG became almost the same as those of the continuous methods (CFI and CGI). The higher recoveries are recorded at early stages for CGI which affect the project economics positively (Zhou et al., 2012) and similar observation is made for CFI. In terms of project economics for a long term, alternating methods (WAGS and

WAG) are favorable because the expenditure required is low as compared to the continuous to achieve similar optimum NPV in the long term.

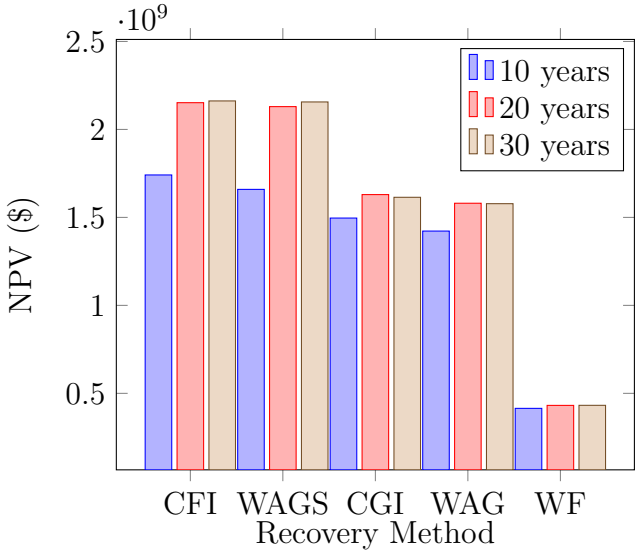

Figure 5.22: NPV for different recovery methods.

Comparisons were made for the different recovery methods for Q_{op}, P_f and η_{op} for 10 years forward model and a similar observation was made as NPV comparisons. CF had the highest NPV followed by WAGS, CGI, WAG and WF for all cases. Figs 5.23 to 5.25 show the Q_{op}, P_f and η_{op} plots respectively.

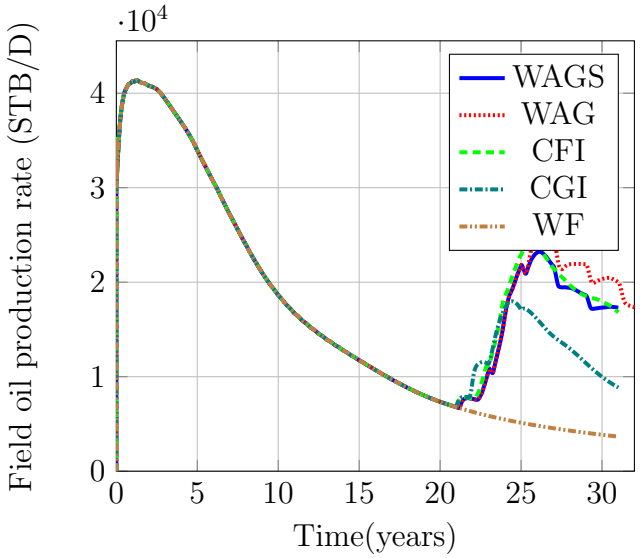

Figure 5.23: FOPR for different recovery methods for 10 years foam flood.

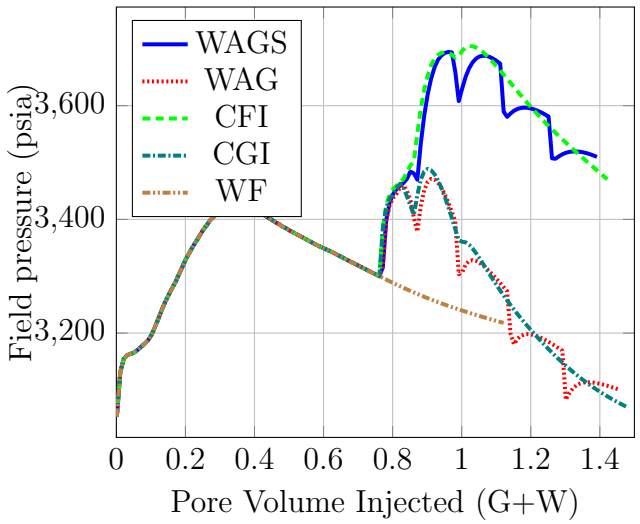

Figure 5.24: FPR for different recovery methods for 10 years foam flood.

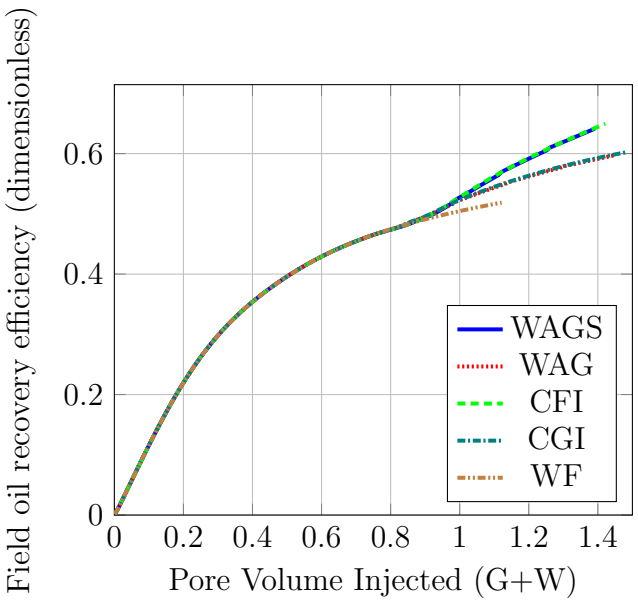

Figure 5.25: FOE for different recovery methods for 10 years foam flood.

CHAPTER 6

FOAM FLOODING OPTIMIZATION

6.1 Optimization

For optimum NPV to be achieved during foam flooding, optimizing foam design parameters is essential. Several design parameters such as surfactant amount, cycle ratio, cycle length, foam quality etc are optimized to achieve optimum NPV. Two different cases were optimized. The reservoir model used was the same as sensitivity study case. The optimization parameters were well locations and cycle ratio. Well locations were determined for x and y coordinates while assuming the wells were completed in all four layers. The minimum and maximum x and y coordinates were based on the grid dimension values (i.e. 1 and 50). For the ratio, it was based on injection period. A minimum of 1 day and a maximum of 700 *days* were used for the determination of water half cycle. The cycle length was fixed

using ECLIPSE simulator keyword DATES. Hence the optimum water injection period determined is subtracted from the cycle length to get gas injection half cycle length. Each optimization process was repeated for 5 realizations to make sure the optimum value is determined

For both cases, total field production and injection rates were used as the primary control and BHP as the secondary control. Total liquid rate target of 100000 STB/D was used as control mode for total field production and minimum of 2700 *psia* used for BHP for all producers. Maximum BHP of 4600 *psia* for all injectors and field injection rate target of 63000 STB/D and 140000 $MSCF/D$ target for water and gas respectively. In both cases, 6 injectors and 9 producers were used. The simulation was run using parallel ECLIPSE-100 simulator.

6.2 Case I

For this case, the field has been under water flooding from the beginning of field development for 21 years as the waterflood could not sustain production. Foam injection was optimized for a 10 year period from this point onward. Two optimization algorithms CMA-ES and DE were utilized in the optimization process. Each algorithm was repeated 5 times to generate 5 realizations of the optimal flood parameters and the results from both were compared with optimum case from the sensitivity study. The optimization was run for 50 iterations each iteration has 8 function evaluations and in all 400 function evaluations for each realization. The number of cycles in the 10 years foam flooding is 5. That is,

2 years cycle length for each cycle. Each cycle is made up of a water injection period and a gas injection period. The total injection periods sum up to 700 days. The optimization algorithm determines the optimum number of days out of the 700 days to inject water for each cycle. The design variables are 5, which is based on the number of cycles for the 10 years of foam flooding.

6.2.1 Net Present Value

After 400 objective function evaluations, a maximum NPV value of $\$1.71E9$ and $\$1.79E9$ were obtained for DE and CMA-ES respectively. A minimum NPV of $\$1.28E9$ was recorded for DE. Figures 6.1 and 6.2 show NPV versus function evaluations for each realization at different function evaluations during optimization for DE and CMA-ES respectively. Almost all the realizations converged around 150 function evaluations. Figure 6.3 shows the optimum NPV comparison for each realization for both algorithms. CMA-ES recorded almost the same NPV ($\$1.79E9$) for all realizations whilst DE recorded different NPV values at each realization. All the NPV values recorded by CMA-ES were above the sensitivity NPV value of $\$1.73E9$ while DE maximum NPV recorded was $\$1.71E9$. In this case the result from the DE were not as good as the NPV obtained from the sensitivity studies.

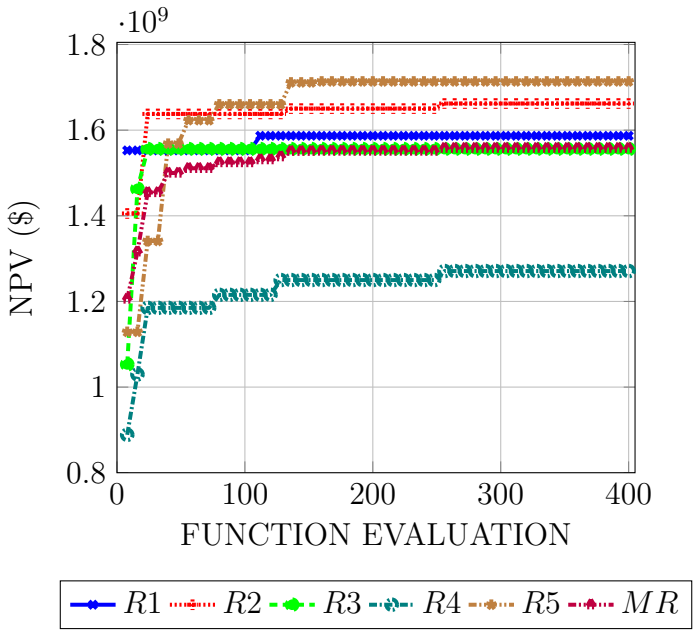

Figure 6.1: NPV versus Function evaluations per realization and mean of 5 realizations for DE.(Case I).

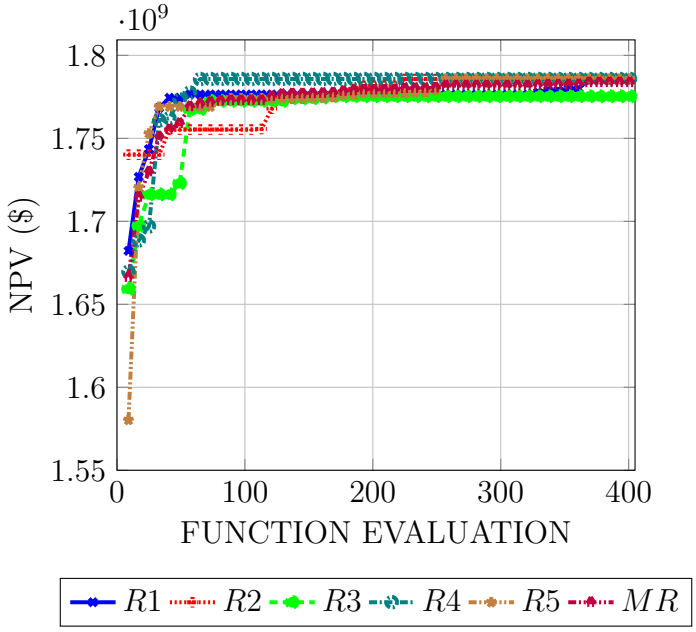

Figure 6.2: NPV versus Function evaluations per realization and mean of 5 realizations for CMA-ES.(Case I).

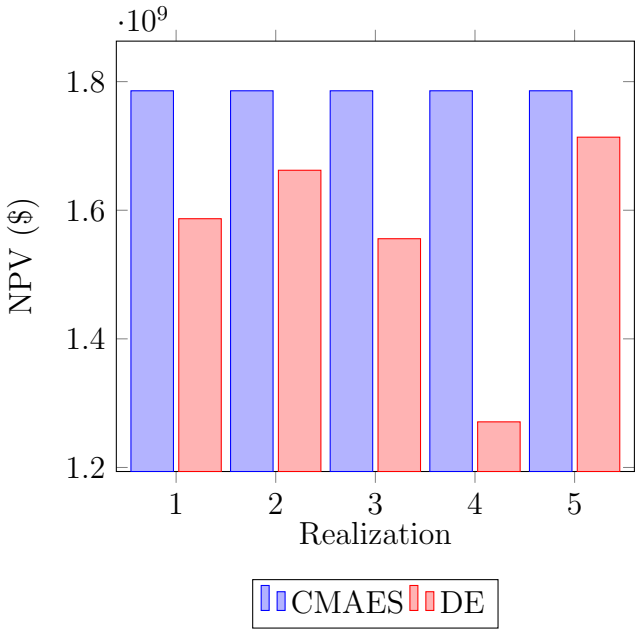

Figure 6.3: Optimum NPV comparisons per realization for Case I

6.2.2 Other Performance Indicators

Optimized Q_{op} by CMA-ES was almost the same as DE for the first 4 years (Fig 6.4). Beyond that period optimized Q_{op} by CMA-ES was higher than that of DE. Almost immediately at the start of foam flooding Q_{op} increased due to the pressure P_f increment as shown in Fig 6.5 and more pore volumes were injected for CMA-ES optimized Q_{op} than DE. In the long run CMA-ES injected more pore volumes than DE leading to higher η_{op} (Fig 6.6). From the optimized period for injection of each phase as shown in Table 6.1 for DE and Table 6.2 for CMA-ES, DE optimized injection periods had long water injection periods as compared to CMA-ES almost zero water injection period for the first four cycles. A minimum of 1 day of water injection period for all cycles was recorded by CMA-ES but 700 days of water injection period for the last cycles. From these CMA-ES results we can infer that for the first 8 years we have continuous foam injection until

the last 2 years when WAGS begins. This possibly explains high NPV recorded for CMA-ES since from the sensitivity study continuous foam injection performs better than WAGS at early stage of foam flooding but WAGS perform better at the later stage. These results may lead us to determine when to start WAGS during foam flooding. For all realizations, CMA-ES recorded the same optimum injection periods but DE had different injection ratios for each realization. DE fifth realization was the best it recorded. A closer look at those values (Table 6.1) for fifth realizations shows low cycle ratio for the first 4 years, that explains why it has similar Q_{op} and P_f as CMA-ES. Q_{op} and P_f for the next four were low because of the high cycle ratio.

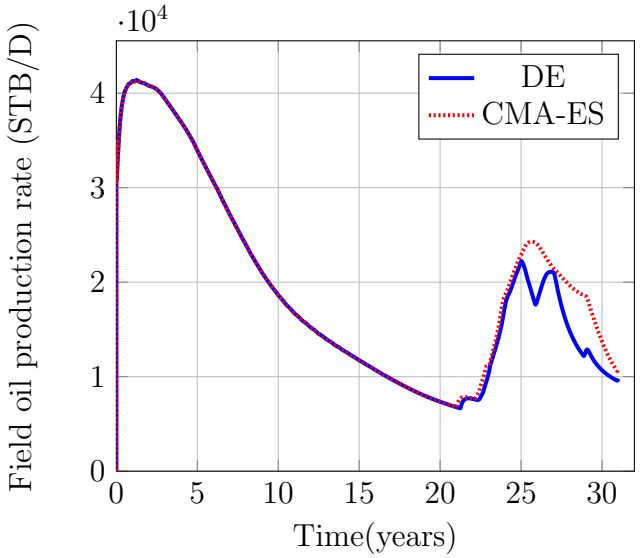

Figure 6.4: Optimized field oil production rate for CASE I

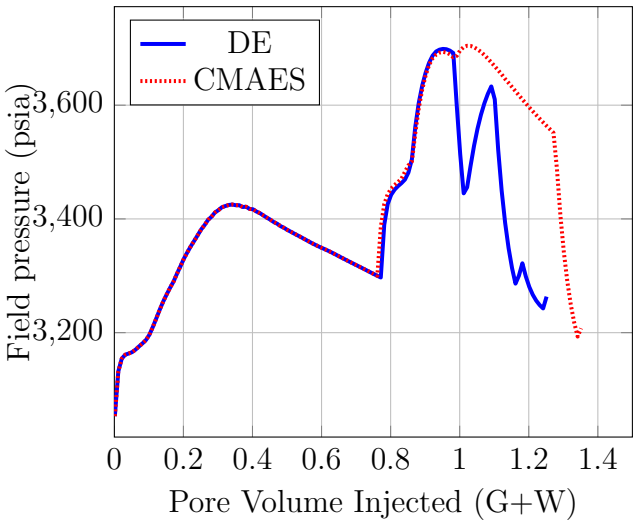

Figure 6.5: Optimized field pressure for CASE I

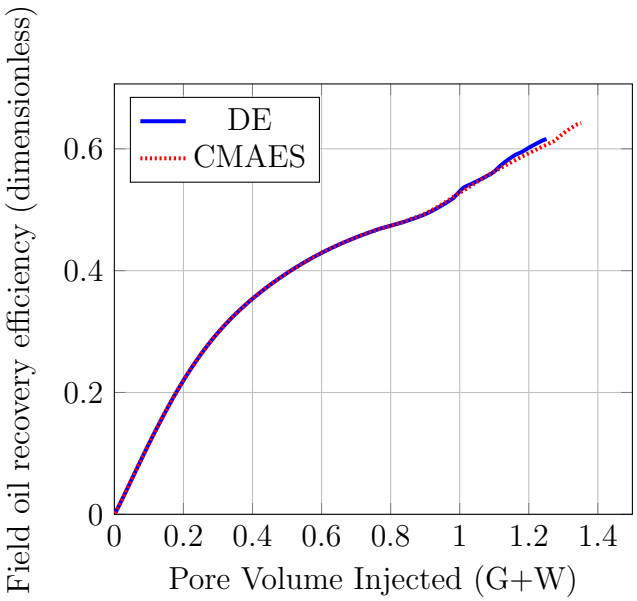

Figure 6.6: Optimized field oil recovery efficiency for CASE I

Table 6.1: Optimized injection period by DE Case I.

Realizations	Cycle Period (days)									
	1		2		3		4		5	
	t_w	t_g	t_w	t_g	t_w	t_g	t_w	t_g	t_w	t_g
1	220	511	553	178	560	171	97	634	155	576
2	74	657	483	248	556	175	239	492	267	464
3	698	33	3	728	493	238	12	719	616	115
4	635	96	598	133	688	43	11	720	177	554
5	90	641	1	730	307	424	676	55	698	33

Table 6.2: Optimized injection period by CMA-ES Case I.

Realizations	Cycle Period (days)									
	1		2		3		4		5	
	t_w	t_g	t_w	t_g	t_w	t_g	t_w	t_g	t_w	t_g
1	1	730	1	730	1	730	1	730	700	31
2	1	730	1	730	1	730	1	730	700	31
3	1	730	1	730	1	730	1	730	700	31
4	1	730	1	730	1	730	1	730	700	31
5	1	730	1	730	1	730	1	730	700	31

6.3 Case II

For this case, the field is assumed to be a newly discovered field. Well locations are optimized for vertical producers and injectors for primary and secondary recovery stages undergoing waterflooding for 21 years. Following the waterflood period, foam was injected for a 10 year period. The foam parameters optimized were the injection periods for water and foam. The number of cycles is the same as presented in Case I. The total number of design variables for this Case is 35, 30 for well locations and 5 for optimum number of days for water injection for each cycle. The design parameters are generated and written to the simulator input file simultaneously. Two optimization algorithms, CMA-ES and DE, were utilized in the optimization process. Each algorithm was repeated for 5 realizations and the results for both compared with optimum case for the sensitivity study. In this section we have three different sub-sections. The first sub-section deals with conventional well placement optimization in heterogeneous reservoir without minimum inter-well distance condition. The second sub-section deals with conventional well optimization in homogeneous reservoir and the third sub-

section introduced a concept in well placement optimization that incorporates a minimum inter-well distance.

6.3.1 Conventional Well Placement Optimization

To determine the location of a well in a discretized reservoir, the optimization algorithms generates x and y coordinates randomly within the reservoir domain. The coordinates are generated between a lower and an upper limit of the discretized dimensions of the reservoir in x and y coordinates. Subsequent locations of the wells are based on the inbuilt optimization mechanism of each algorithm. After running 5 realizations both algorithms recorded a mean NPV of $\$8.1E9$. Figures 6.7 and 6.8 show the NPV versus objective function evaluations for CMA-ES and DE respectively.

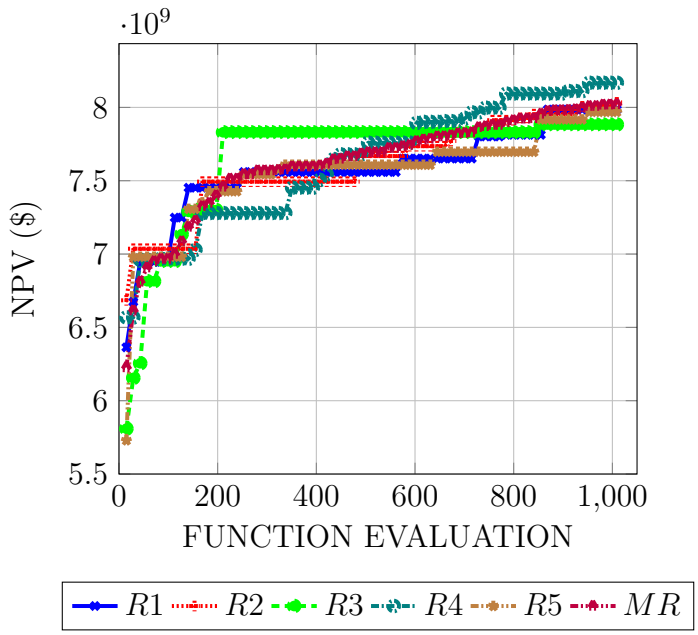

Figure 6.7: NPV versus objective function evaluations for 9 realizations and mean realizations Case II (CMA-ES).

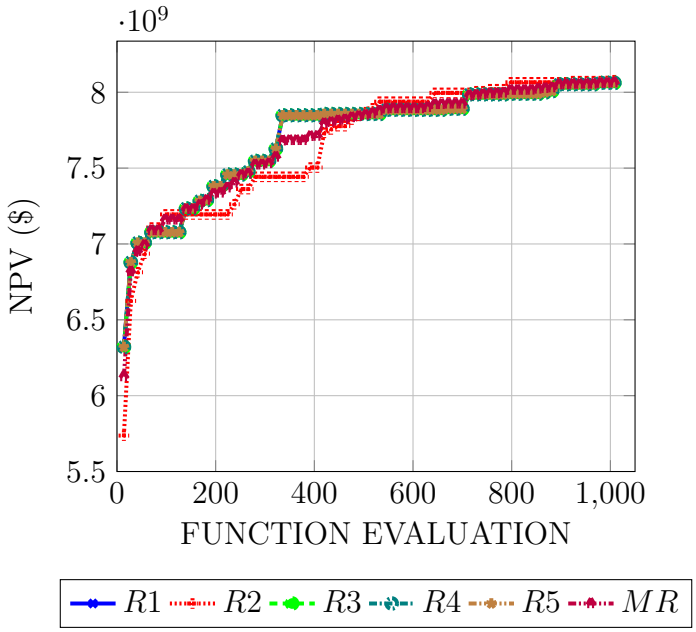

Figure 6.8: NPV versus objective function evaluations for 9 realizations and mean realizations Case II (DE).

One major challenge with these optimization algorithms is their inability to enforce minimum inter-well distance during well placement optimization. Making decisions based on only the highest NPV recorded could sometimes be misleading, though NPV is the objective function being maximized. To eliminate such solutions, the minimum safe distance around each well is assumed to be 10 $acres$ which translates to a circular radius of 372 ft. Since each grid block size is 260 ft in both x and y directions, for any optimum solution from the algorithm to be accepted, any pair of wells should have at least an inter-well distance of 372 ft in between them. Hence a minimum of two grid blocks should be between two neighboring wells, else that particular solution is rejected. Figures 6.9 and 6.10 show optimum well locations for best realizations for CMA-ES and DE respectively. From these Figs the wells are well spaced and the problem of having wells

that are too close did not occur. However, in Fig 6.9, where the well configuration from a realization from CMA-ES is presented, producers 5 and 8 are seen to be too close. A similar scenario is observed in Fig 6.10 representing the outcome of a realization from DE. In this case, producers 3 and 8 are very close to each other. This form the basis to consider a homogeneous reservoir case to figure out if that behavior of having wells too close to each other is due to the heterogeneity.

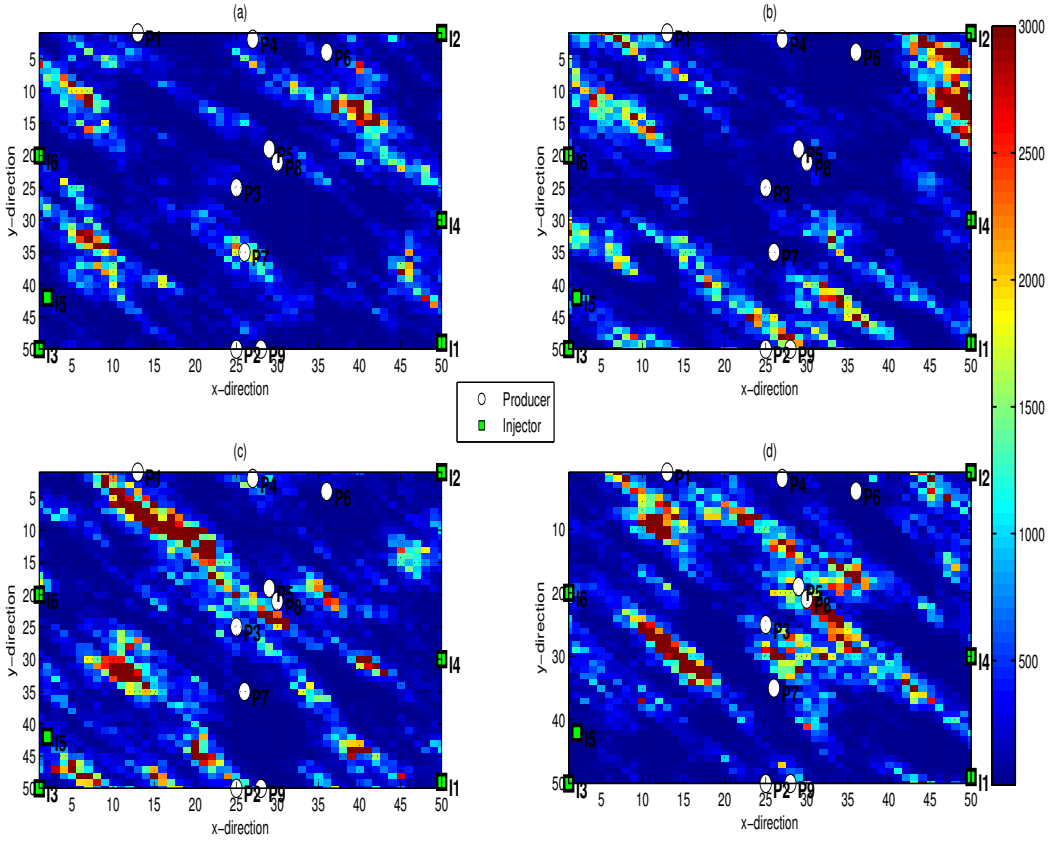

Figure 6.9: Optimized well locations Case II (a) Layer 1 (b) Layer 2 (c) Layer 3 (d) Layer 4 (R2-CMA-ES).

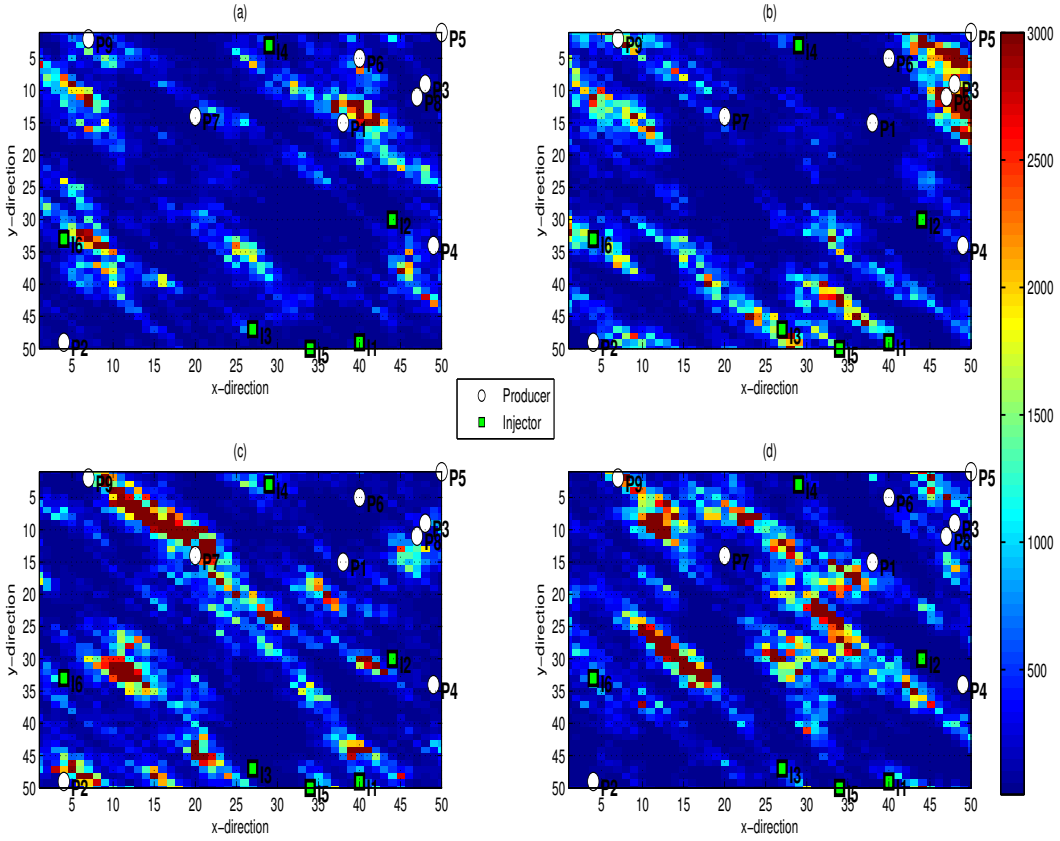

Figure 6.10: Optimized well locations Case II (a) Layer 1 (b) Layer 2 (c) Layer 3 (d) Layer 4 (R2-DE).

Apart from the well locations, injection periods for water and foam were optimized. The optimized period for injecting each phase for each realization is shown in Tables 6.3 and 6.4 for CMA-ES and DE respectively. One inference that can be drawn from these tables is that, the optimum cycle ratio (t_w/t_g) for a particular reservoir is dependent to some extent on the well locations. The same reservoir model was used for both cases I and II. In all cases, the optimum cycle ratio obtained by the different well locations was different for each algorithm. In case I, CMA-ES in all realizations gave the same optimum cycle ratio but gave different cycle ratio when the well locations were changed.

Table 6.3: Optimized injection periods for heterogeneous reservoir with no inter well distance Case II (CMA-ES).

Realizations	Cycle Period (days)									
	1		2		3		4		5	
	t_w	t_g	t_w	t_g	t_w	t_g	t_w	t_g	t_w	t_g
1	638	93	107	624	700	31	325	406	84	647
2	378	353	1	730	700	31	80	651	96	635
3	511	220	580	151	7	724	62	669	260	471
4	405	326	1	730	159	572	384	347	108	623
5	158	573	46	685	207	524	598	133	700	31

Table 6.4: Optimized injection periods for heterogeneous reservoir with no inter well distance Case II (DE).

Realizations	Cycle Period (days)									
	1		2		3		4		5	
	t_w	t_g	t_w	t_g	t_w	t_g	t_w	t_g	t_w	t_g
1	191	540	225	506	693	38	27	704	24	707
2	656	75	601	130	31	700	160	571	332	399
3	511	220	580	151	7	724	62	669	260	471
4	191	540	225	506	693	38	27	704	24	707
5	191	540	225	506	693	38	27	704	24	707

6.3.2 Homogeneous Reservoir Model

As observed in Figs 6.12 and 6.13, the optimization process was repeated on a homogeneous reservoir model. The permeability and porosity of this model were chosen based on volume average. DE algorithm which had majority of the optimum solutions generated having these wells close to each other was the only algorithm implemented. After running DE 5 times to generate 5 realizations, it was observed that, about 40% of the optimum solutions generated had wells too close to each other. Figures 6.12 and 6.13 show the solutions with this challenge of wells too close to each other. An inference can be drawn here that, heterogeneity also plays part in generating these types of solutions. Even though the mean of the optimum NPV's is $\$8.8E9$ as in Fig 6.11 higher than the heterogeneous case. Since the problem still persists, we tried a new concept with minimum inter-well distance. This concept is addressed in the next sub-section. A look at the optimum injection period (Table 6.5) for each cycle shows more water injection period as in Case I. This is due to fact that most of producers are at the peripherals of the reservoir which results in less oil sweep efficiency.

Table 6.5: Optimized injection periods for homogeneous reservoir with no inter well distance.

Realizations	Cycle Period (days)									
	1		2		3		4		5	
	t_w	t_g	t_w	t_g	t_w	t_g	t_w	t_g	t_w	t_g
1	257	474	360	371	613	118	32	699	2	729
2	700	31	191	540	698	33	249	482	674	57
3	4	727	657	74	469	262	78	653	419	312
4	219	512	19	712	682	49	43	688	10	721
5	699	32	216	515	436	295	694	37	585	146

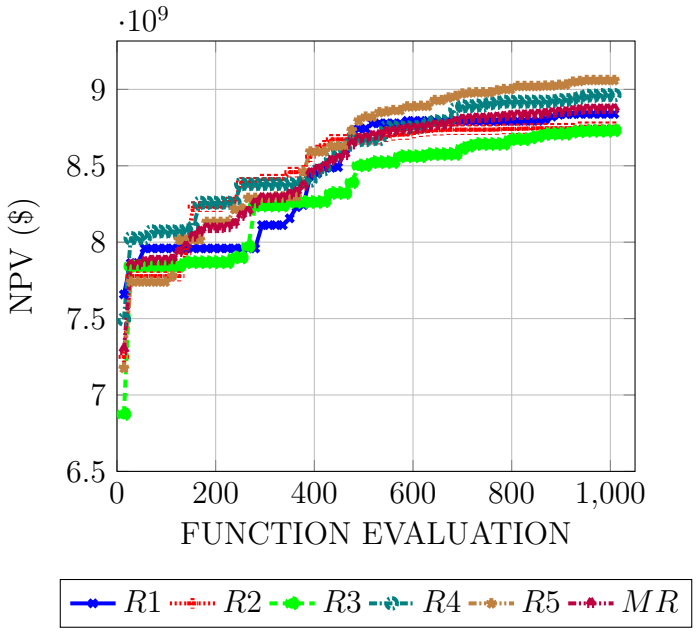

Figure 6.11: NPV versus objective function evaluations for 5 realizations and mean realizations Homogeneous Case.

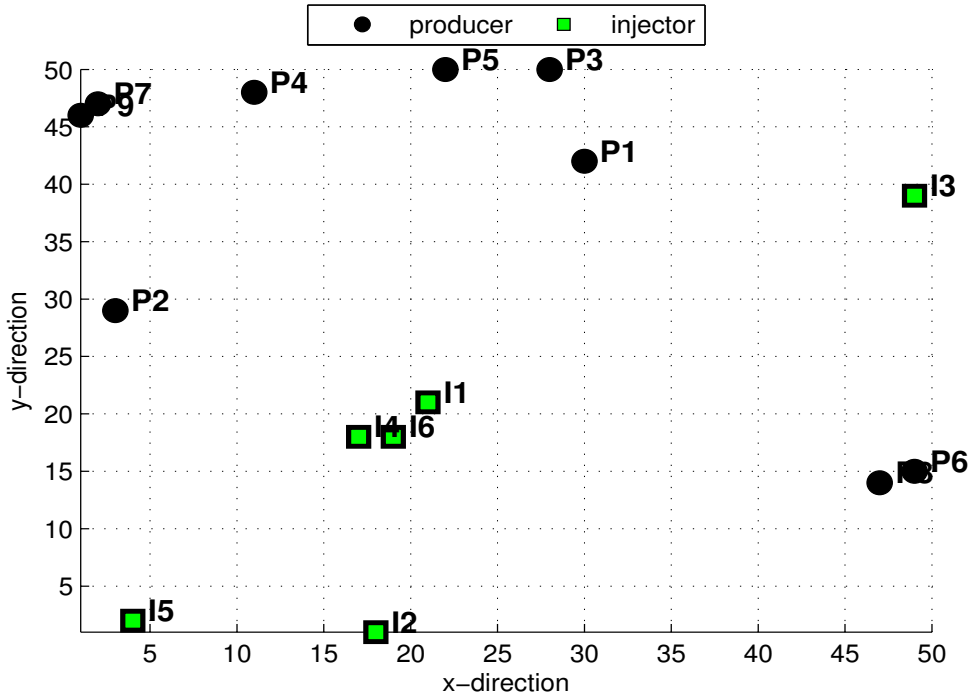

Figure 6.12: Optimized well locations for homogeneous reservoir (R1).

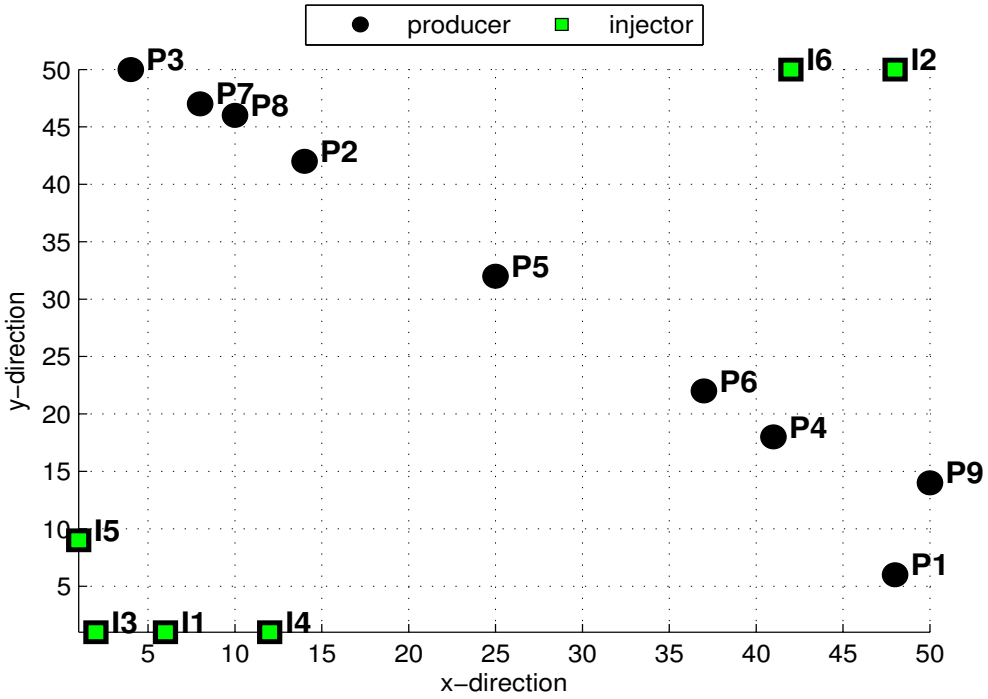

Figure 6.13: Optimized well locations for homogeneous reservoir (R5).

6.3.3 Enforcing Minimum Inter-Well Spacing in Well Placement Optimization

We adopt a method that enforces a minimum well spacing between wells. The method involves changing the way random numbers are generated between the lower and upper limits of the search space.

Assuming that, to ensure minimum safe distance of 1000 ft between 2 wells in a reservoir of dimension $50 \times 50 \times 4$. Each grid block has a size of 260 ft in x and y directions. That means at least 4 gridblocks should be between 2 neighboring wells in the reservoir. In our procedure, this means;

- We divide the upper limits of both x and y which is 50 by 4 to get a new upper limit of 12.5.
- The algorithm now generates randomly numbers between 1 to 12.5 instead of 1 to 50.
- The randomly generated numbers between 1 to 12.5 are multiplied by 4 to keep a differnce of 4 between 2 close numbers.

These new numbers are used as the coordinates of well in the reservoir that ensures a minimum inter-well distance is kept between 2 neighboring wells in the reservoir. To see the effect of having all even locations and both even and odd solutions searched, we optimized a minimum inter-well distance of 910 ft and 1000 ft. These distances translate to 3.5 and 4 respectively. After 5 realizations, the observed mean NPV for both minimum inter-well distance of 910 ft and

1000 ft was \$7.7E9 and \$7.6E9 respectively for CMA-ES and \$7.8E9 for both inter-well distances for DE. These mean optima NPV are comparable with the case without minimum inter-well distances mean NPV of \$8.0E9. Figures 6.15 to 6.16 show NPV for each realization for CMA-ES and DE respectively for 910 ft and 1000 ft.

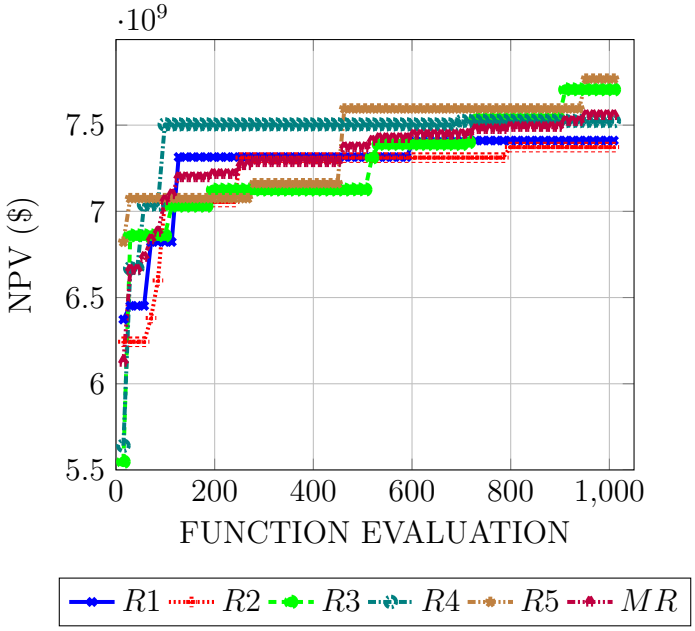

Figure 6.14: NPV versus objective function evaluation for minimum inter-well distance of 910 ft (CMA-ES).

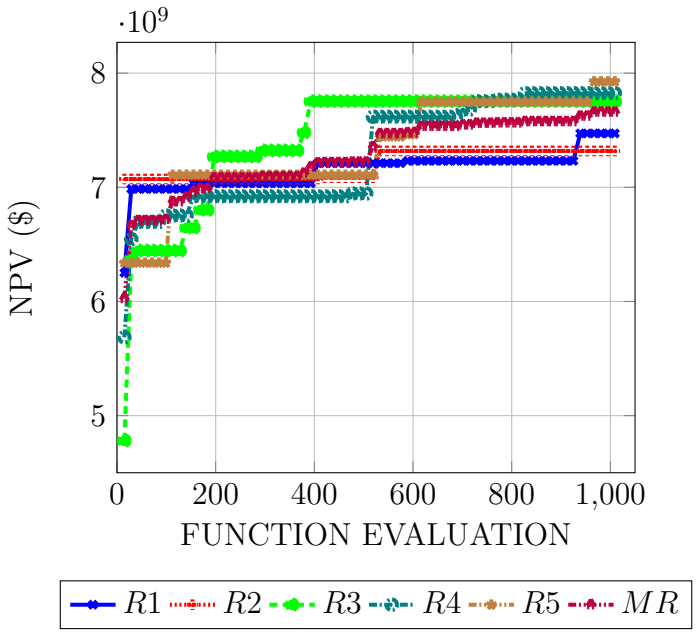

Figure 6.15: NPV versus objective function evaluation for minimum inter-well distance of 1000 ft (CMA-ES).

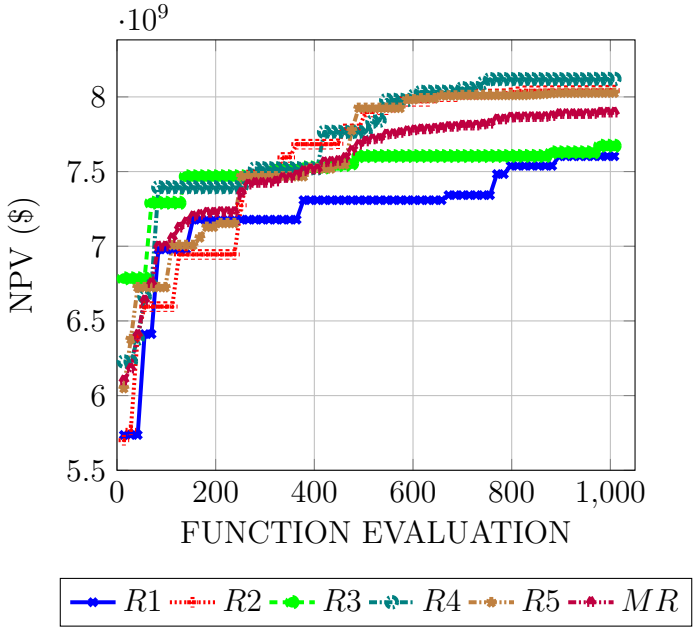

Figure 6.16: NPV versus objective function evaluation for minimum inter-well distance of 910 ft (DE).

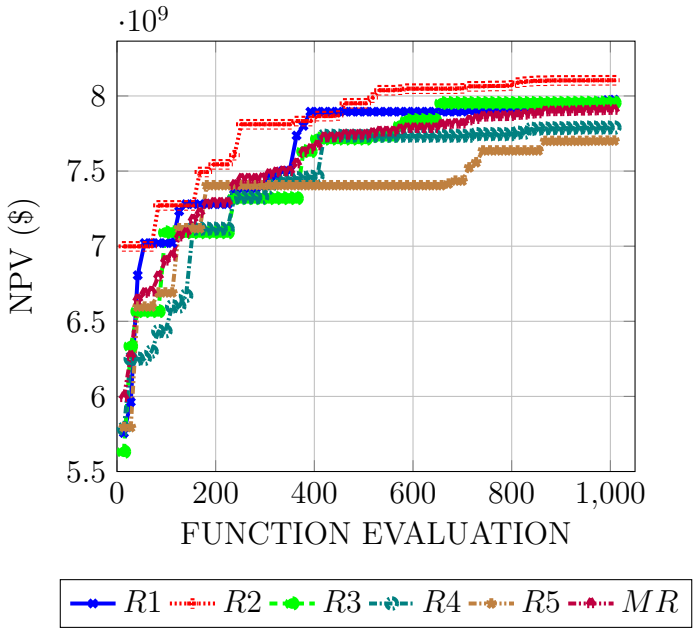

Figure 6.17: NPV versus objective function evaluation for minimum inter-well distance of 1000 ft (DE).

Well locations generated for the optima solutions for this new concept incorporates minimum inter-well distance when optimizing well locations which are close to each other (Figs 6.18 to 6.21). In Fig 6.20 , producers 5 and 7 though closer but kept a minimum distance of 900 ft for CMA-ES. The same can be said of producers 3 and 7 in Figure 6.21 for DE. A minimum inter-well distance of 1000 ft is kept for producers 4 and 8 and producers 6 and 9 as observed in Figs 6.20 and 6.21 for CMA-ES and DE respectively. This new concept is applicable when specified minimum inter-well distance in field development must be observed.

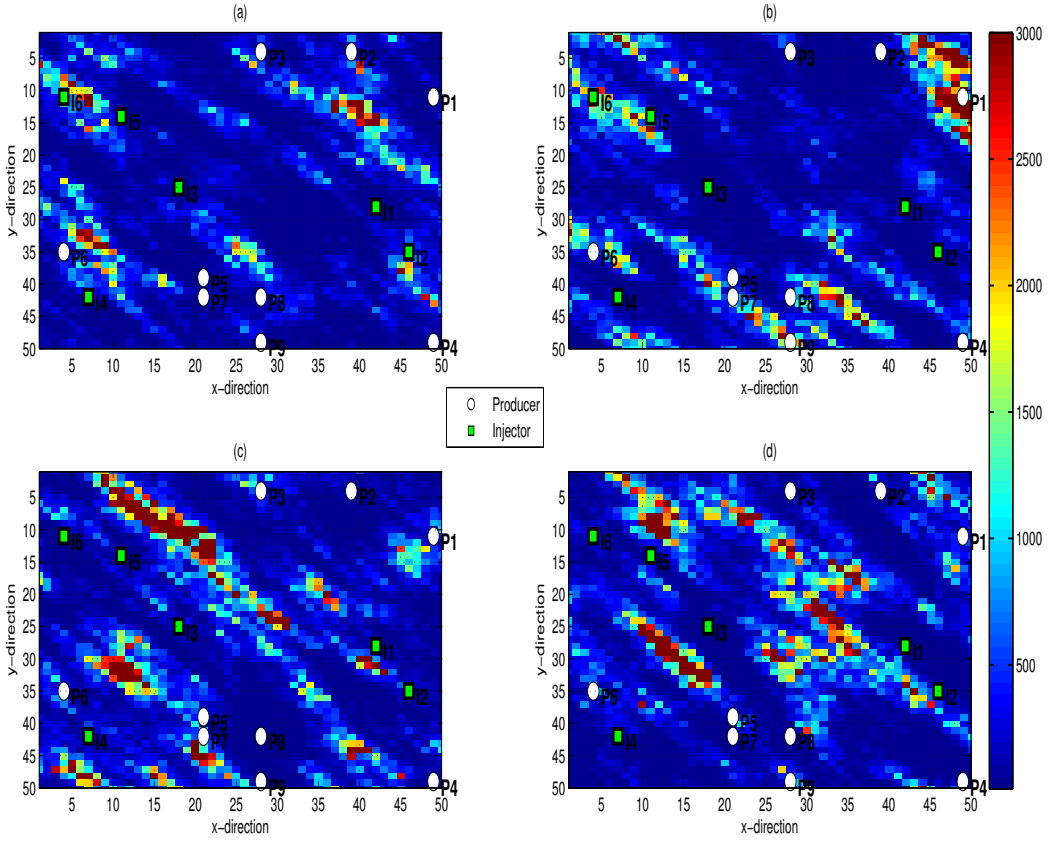

Figure 6.18: Optimum well locations for minimum inter-well distance of 1000 ft (a) Layer 1 (b) Layer 2 (c) Layer 3 (d) Layer 4 (R2-CMA-ES).

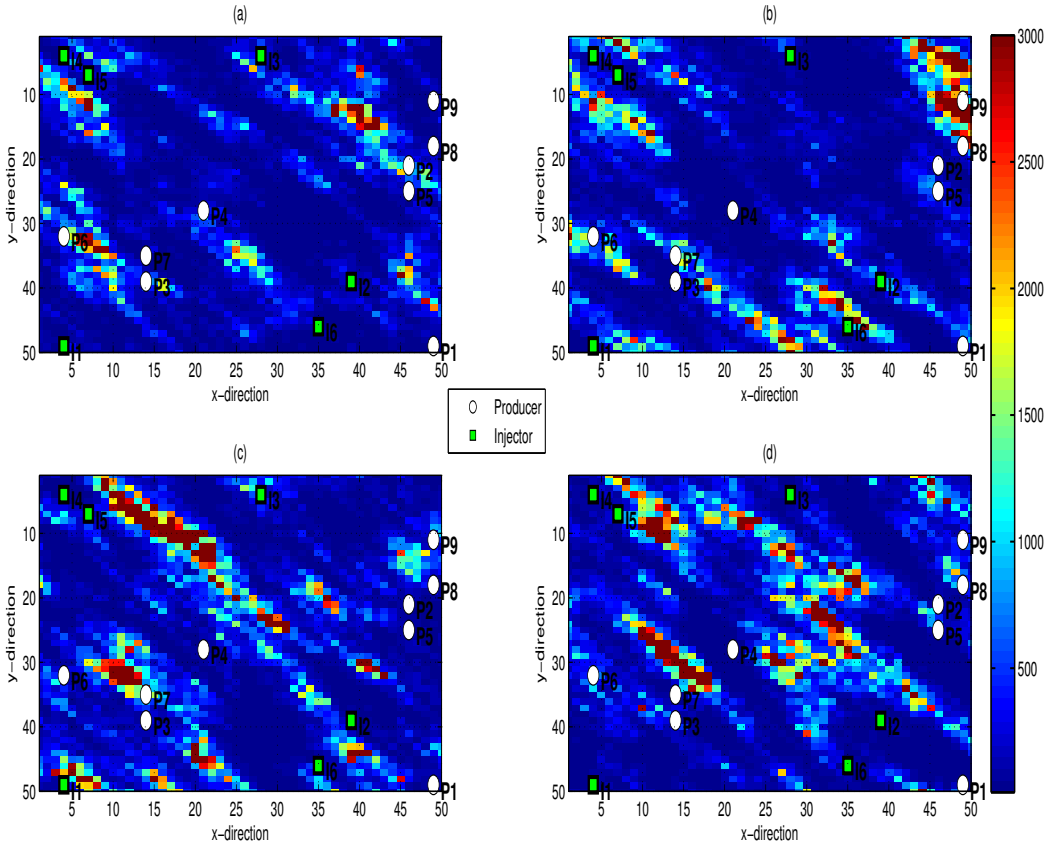

Figure 6.19: Optimum well locations for minimum inter-well distance of 900 ft (a) Layer 1 (b) Layer 2 (c) Layer 3 (d) Layer 4 (DE).

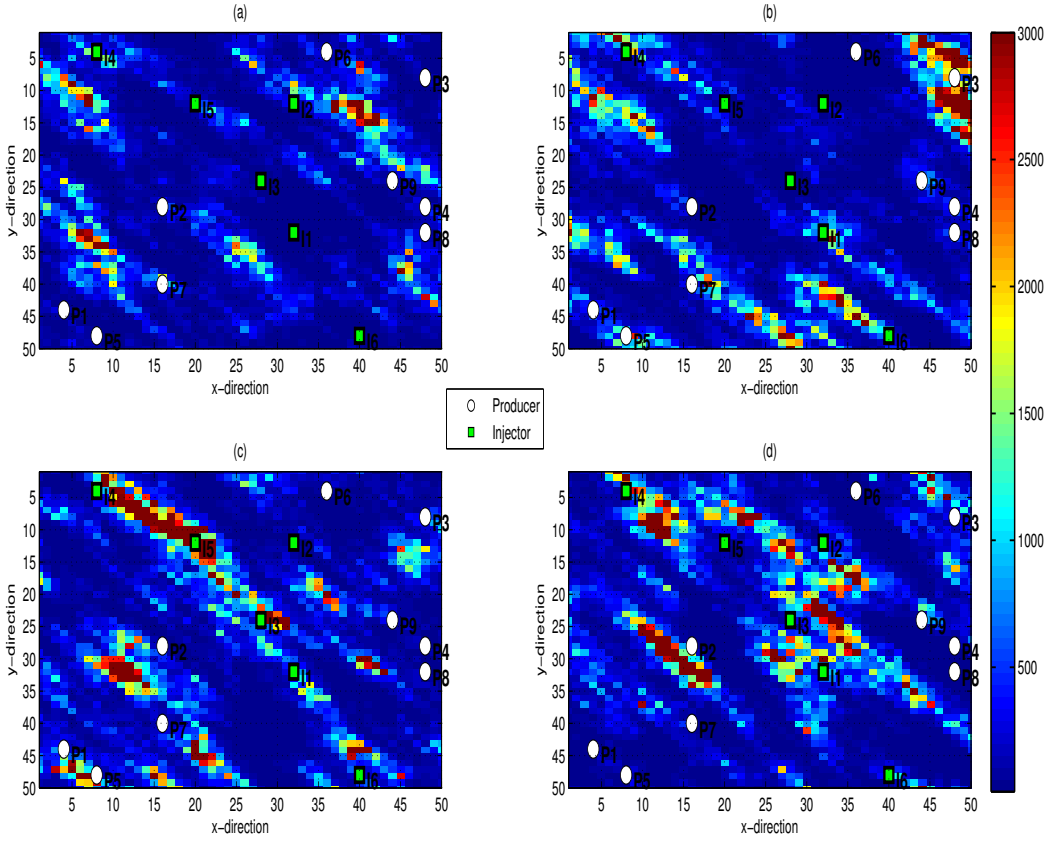

Figure 6.20: Optimum well locations for minimum inter-well distance of 900 ft (a) Layer 1 (b) Layer 2 (c) Layer 3 (d) Layer 4 (CMA-ES).

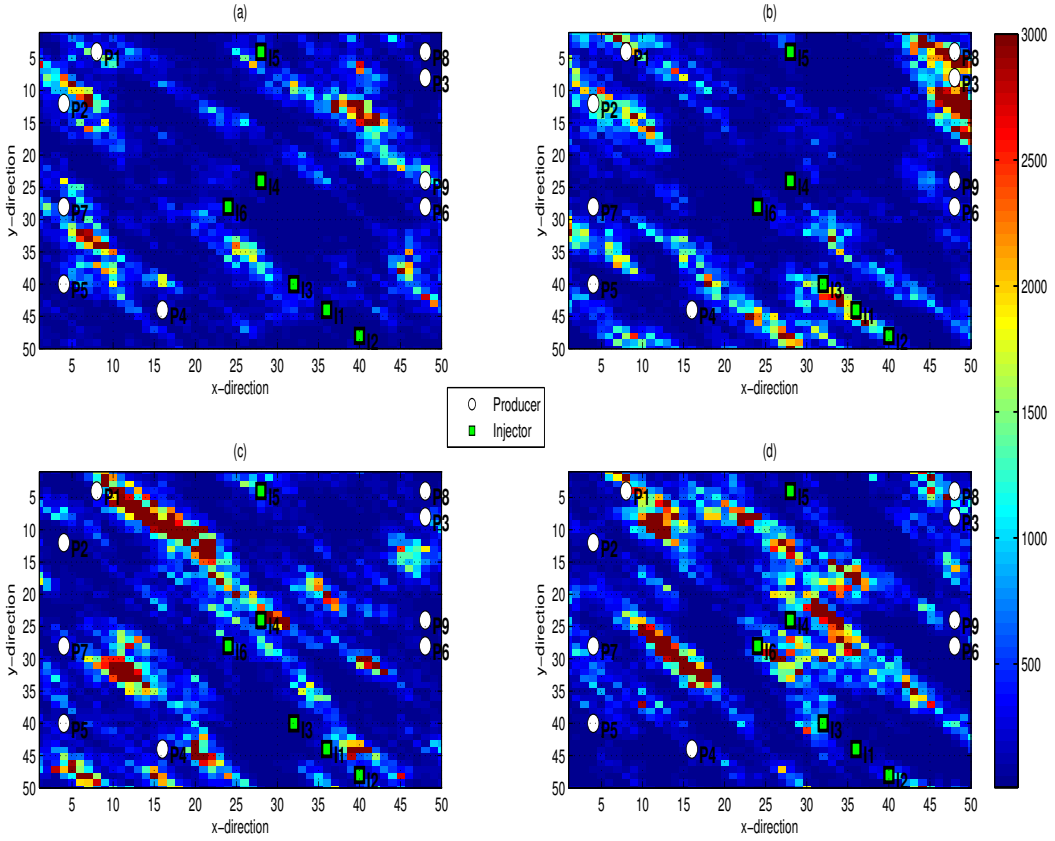

Figure 6.21: Optimum well locations for minimum inter-well distance of 1000 ft (a) Layer 1 (b) Layer 2 (c) Layer 3 (d) Layer 4 (DE).

Tables 6.6 to 6.9 show optimum injection periods for the cases in which minimum inter-well distance of 900 ft and 1000 ft were enforced respectively. A careful look at these tables show more water alternating gas unlike Case I which had CFI in first 8 years before WAGS in the last two years. This behavior may be attributed to locations of the wells. The producers in Case I are distributed evenly inside the reservoir with the injectors at the peripherals. In this new concept the producers are located inside the reservoir unlike the conventional case we still have the challenge of the injectors also located inside and some times aligning them selves closer to each other which leaves a lot of unswept area in the reservoir. This may also account for high water injection periods since the waterflooding is less expensive as compared with gas.

Table 6.6: Optimized injection periods for heterogeneous reservoir with inter well distance of 1000 ft (DE).

Realizations	Cycle Period (days)									
	1		2		3		4		5	
	t_w	t_g	t_w	t_g	t_w	t_g	t_w	t_g	t_w	t_g
1	25	706	88	643	645	86	427	304	237	494
2	135	596	24	707	466	265	417	314	419	312
3	482	249	72	659	81	650	542	189	259	472
4	346	385	700	31	578	153	162	569	210	521
5	700	31	1	730	268	463	278	453	663	68

Table 6.7: Optimized injection periods for heterogeneous reservoir with inter well distance of 1000 ft (CMA-ES).

Realizations	Cycle Period (days)									
	1		2		3		4		5	
	t_w	t_g	t_w	t_g	t_w	t_g	t_w	t_g	t_w	t_g
1	6	725	529	202	429	302	57	674	1	730
2	1	730	5	726	2	729	1	730	574	157
3	19	712	578	153	451	280	698	33	214	517
4	586	145	542	189	8	723	73	658	1	730
5	5	726	699	32	451	280	283	448	369	362

Table 6.8: Optimized injection periods for heterogeneous reservoir with inter well distance of 910 ft (DE).

Realizations	Cycle Period (days)									
	1		2		3		4		5	
	t_w	t_g	t_w	t_g	t_w	t_g	t_w	t_g	t_w	t_g
1	617	114	227	504	700	31	539	192	1	730
2	588	143	220	511	700	31	449	282	87	644
3	1	730	292	439	248	483	472	259	652	79
4	700	31	1	730	40	691	700	31	286	445
5	1	730	403	328	447	284	510	221	134	597

Table 6.9: Optimized injection periods for heterogeneous reservoir with inter well distance of 910 ft (CMA-ES).

Realizations	Cycle Period (days)									
	1		2		3		4		5	
	t_w	t_g	t_w	t_g	t_w	t_g	t_w	t_g	t_w	t_g
1	435	296	146	585	644	87	577	154	574	157
2	595	136	5	726	58	673	687	44	678	53
3	27	704	317	414	1	730	118	613	414	317
4	628	103	1	730	108	623	212	519	21	710
5	1	730	402	329	9	722	684	47	331	400

CHAPTER 7

CONCLUSIONS

7.1 Conclusions

From the above study, we draw the following conclusions;

- Continuous foam injection is profitable at the early stage but decreases in profitability when the project life is long as compared to alternating foam injection.
- When implementing cycling foam injection, cycle ratio has more effect on final profitability of the project.
- Cycle length has no effect on profitability of foam flooding project.
- Lower cycle ratio has higher recovery than high cycle ratio.
- Optimum cycle ratio is between 0.5 and 1.
- Cycle ratios below 0.5 have higher recovery at early stage of foam project but

efficiency decreases at later stage since below 0.5 ratio is closer to continuous foam flooding.

- Well locations of a field influence the optimum cycle ratio during foam flooding.
- A concept of optimizing well locations have been developed which takes into account minimum inter-well distance.

Bibliography

Almehaideb, R. A., Shedid, S. A. and Zekri, A. Y. (2008), Laboratory study of miscible carbon dioxide flooding of uae carbonate oil reservoirs, Society of Petroleum Engineers, Abu Dhabi, UAE.

Andrianov, A., Farajzadeh, R., Nick, M. M., Talanana, M. and Zitha, P. L. (2011), Immiscible foam for enhancing oil recovery: Bulk and porous media experiments, Society of Petroleum Engineers, Kuala Lumpur, Malaysia.

Arshad, A., Al-Majed, A. A., Menouar, H., Muhammadain, A. M. and Mtawaa, B. (2009), Carbon dioxide (co_2) miscible flooding in tight oil reservoirs: A case study, Society of Petroleum Engineers, Kuwait City, Kuwait.

Asghari, K. and Torabi, F. (2008), Effect of miscible and immiscible co_2 flooding on gravity drainage: Experimental and simulation results, Society of Petroleum Engineers, Tulsa, Oklahoma, USA.

Bai, B., Grigg, R., Liu, Y. and Zeng, Z.-W. (2005), Adsorption kinetics of surfactant used in co_2-foam flooding onto berea sandstone, Society of Petroleum Engineers, Dallas, Texas.

Barnawi, M. T. (2008), A Simulation Study to verify Stone's Simultaneous Water and Gas Injection Injection Performance In 5-Spot Pattern, PhD thesis, Texas A & M University, College Station.

Bender, S. (2011), Co-Optimization of CO_2 Sequestration and Enhanced Oil Recovery and Co-Optimization of $CO-2$ Sequetration and Methane Recovery in Geopressured Aquifers, PhD thesis, University of Texas, Austin.

Bian, Y., Penny, G. S. and Sheppard, N. C. (2012), Surfactant formulation evaluation for carbon dioxide foam flooding in heterogeneous sandstone reservoir, Society of Petroleum Engineers, Tulsa, Oklahoma, USA.

Blaker, T., Celius, H., Lie, T., Martinsen, H., Rasmussen, L. and Vassenden, F. (1999), Foam for gas mobility control in the snorre field: The fawag project, Society of Petroleum Engineers, Houston, Texas.

Bouzarkouna, Z., Ding, Y. D. and Auger, A. (2011), Partially separated metamodels with evolution strategies for well placement optimization, Society of Petroleum Engineers, Vienna, Austria.

Chang, S.-H. and Grigg, R. B. (1998), Effects of foam quality and flow rate on co_2-foam behavior at reservoir conditions, Society of Petroleum Engineers, Tulsa, Oklahoma.

Chen, S., Li, H., Yang, D. and Tontiwachwuthikul, P. (2009), Optimal parametric design for water- alternating-gas (wag) process in a co_2 miscible flooding reservoir, Petroleum Society of Canada, Calgary, Alberta.

Chen, S., Li, H., Yang, D. and Tontiwachwuthikul, P. (2010), 'Optimal parametric design for water-alternating-gas (wag) process in a co_2-miscible flooding reservoir', *Journal of Canadian Petroleum Technology* **49**, pp. 75–82.

Enick, R. M., Olsen, D. K., Ammer, J. R. and Schuller, W. (2012), Mobility and conformance control for co_2 eor via thickeners, foams, and gels – a literature review of 40 years of research and pilot tests, Society of Petroleum Engineers, Tulsa, Oklahoma, USA.

Farajzadeh, R., Andrianov, A. and Zitha, P. L. J. (2009), Foam assisted enhanced oil recovery at miscible and immiscible conditions, Society of Petroleum Engineers, Kuwait City, Kuwait.

Fjelde, I., Zuta, J. and Duyilemi, O. V. (2008), Oil recovery from matrix during co_2-foam flooding of fractured carbonate oil reservoirs, Society of Petroleum Engineers, Rome, Italy.

Fjelde, I., Zuta, J. and Hauge, I. (2009), 'Retention of co_2-foaming agents onto chalk: Effects of surfactant structure, temperature, and residual-oil saturation', *SPE Reservoir Evaluation & Engineering* **12**, pp. 419–426.

Gao, P., Towler, B. F. and Jiang, H. (2010), Feasibility investigation of co_2 miscible flooding in south slattery minnelusa reservoir, wyoming, Society of Petroleum Engineers, Anaheim, California, USA.

Ghedan, S. G. (2009), Global laboratory experience of co_2-eor flooding, Society of Petroleum Engineers, Abu Dhabi, UAE.

Ghomian, Y., Pope, G. A. and Sepehrnoori, K. (2008), Hysteresis and field-scale optimization of wag injection for coupled co_2-eor and sequestration, Society of Petroleum Engineers, Tulsa, Oklahoma, USA.

Grigg, R. B. and Mikhalin, A. A. (2007), Effects of flow conditions and surfactant availability on adsorption, Society of Petroleum Engineers, Houston, Texas, U.S.A.

Grigg, R. B., Tsau, J.-S. and Martin, F. D. (2002), Cost reduction and injectivity improvements for co_2 foams for mobility control, 2002,. Society of Petroleum Engineers Inc., Tulsa, Oklahoma.

Guo, X., Du, Z., Sun, L., Huang, W. and Zhang, C. (2006), Optimization of tertiary water-alternate-co_2 flood in jilin oil field of china: Laboratory and simulation studies, Society of Petroleum Engineers, Tulsa, Oklahoma, USA.

Guzman, R., Giordano, D., Fayers, F., Aziz, K. and Godi, A. (1994), Three-phase flow in field-scale simulations of gas and wag injections, Copyright 1994, Society of Petroleum Engineers Inc., London, United Kingdom.

Hajizadeh, Y., Christie, M. A. and Demyanov, V. (2010), History matching with differential evolution approach; a look at new search strategies, Society of Petroleum Engineers, Barcelona, Spain.

Hansen, N. and Ostermeier, A. (2001), 'Completely derandomized self-adaptation in evolution strategies', *Evolutionary Computation* **9**(2), 159–195.

Harding, T., Radcliffe, N. and King, P. (1998), 'Hydrocarbon production scheduling with genetic algorithms', *SPE Journal* **3**, 99–107.

Jahangiri, H. R. and Zhang, D. (2011), Optimization of the net present value of carbon dioxide sequestration and enhanced oil recovery, Houston, Texas, USA.

Jiang, H., Nuryaningsih, L. and Adidharma, H. (2012), The study of timing of cyclic injections in miscible co_2 wag, Society of Petroleum Engineers, Bakersfield, California, USA.

Kloet, M., Renkema, W. J. and Rossen, W. R. (2009), Optimal design criteria for sag foam processes in heterogeneous reservoirs, Society of Petroleum Engineers, Amsterdam, The Netherlands.

Kulkarni, M. M. and Rao, D. N. (2005), 'Experimental investigation of miscible and immiscible water-alternating-gas (wag) process performance', *Journal of Petroleum Science and Engineering* **48**, 1–20.

LE, V. Q., Nguyen, Q. P. and Sanders, A. (2008), A novel foam concept with co_2 dissolved surfactants, Society of Petroleum Engineers, Tulsa, Oklahoma, USA.

Mirkalaei, S. M. M., Hoseini, J., Masoudi, R., Ataei, A., Demiral, B. and Karkooti, H. (2011), Investigation of different i-wag schemes toward optimization of displacement efficiency, Society of Petroleum Engineers, Kuala Lumpur, Malaysia.

Mungan, N. (1981), 'Carbon dioxide flooding-fundamentals', *Journal of Canadian Petroleum Technology* **20**.

Odi, U. and Gupta, A. (2010), Optimization and design of carbon dioxide flooding, Society of Petroleum Engineers, Abu Dhabi, UAE.

Odi, U., Lane, R. H. and Barrufet, M. A. (2010), Ensemble based optimization of eor processes, Society of Petroleum Engineers, Anaheim, California, USA.

Onwunalu, J. and Durlofsky, L. (2010), 'Application of a particle swarm optimization algorithm for determining optimum well location and type', *Computational Geosciences* **14**, 183–198.

Oskay, M. M., Al-Shehri, D. A., Abu-Khamsin, S. A. and Marhoun, M. A. (1989), 'Carbon dioxide minimum miscibility pressure for saudi arabian crudes', *The Arabian Journal for Science and Engineering* **14**, 169–180.

Ren, G., Zhang, H. and Nguyen, Q. P. (2011), Effect of surfactant partitioning between co_2 and water on co_2 mobility control in hydrocarbon reservoirs, 2011, Society of Petroleum Engineers, Kuala Lumpur, Malaysia.

Schlumberger (2010), *Eclipse Technical Description Manual*, Houston, Texas.

Shedid, S. A. (2009), 'Influences of different modes of reservoir heterogeneity on performance and oil recovery of carbon dioxide miscible flooding', *Journal of Canadian Petroleum Technology* **48**, 29–36.

Shedid, S. A., Zekri, A. Y. and Almehaideb, R. A. (2008), Optimization of carbon dioxide flooding for a middle-eastern heterogeneous oil reservoir, Petroleum Society of Canada, Calgary, Alberta.

Shi, J.-X. and Rossen, W. (1998), 'Simulation and dimensional analysis of foam processes in porous media', *SPE Reservoir Evaluation & Engineering* **1**, 148–154.

Shoaib, S. and Hoffman, B. T. (2009), co_2 flooding the elm coulee field, Society of Petroleum Engineers, Denver, Colorado.

Skauge, A., Aarra, M., Surguchev, L., Martinsen, H. and Rasmussen, L. (2002), Foam-assisted wag: Experience from the snorre field, Copyright 2002, Society of Petroleum Engineers Inc., Tulsa, Oklahoma.

Skoreyko, F. A., Villavicencio, A. P., Prada, H. R. and Nguyen, Q. P. (2011), Development of a new foam eor model from laboratory and field data of the naturally fractured cantarell field, Society of Petroleum Engineers, Abu Dhabi, UAE.

Skoreyko, F. A., Villavicencio, A. P., Prada, H. R. and Nguyen, Q. P. (2012), Understanding foam flow with a new foam eor model developed from laboratory and field data of the naturally fractured cantarell field, Society of Petroleum Engineers, Tulsa, Oklahoma, USA.

Spirov, P., Rudyk, S. and Khan, A. (2012), Foam assisted wag, snorre revisit with new foam screening model, Society of Petroleum Engineers, Cairo, Egypt.

Storn, R. (1996), On the usage of differential evolution for function optimization, *in* 'Fuzzy Information Processing Society, 1996. NAFIPS., 1996 Biennial Conference of the North American', pp. 519–523.

Storn, R. and Price, K. (1996), Minimizing the real functions of the icec'96 contest by differential evolution, *in* 'Evolutionary Computation, 1996., Proceedings of IEEE International Conference on', pp. 842–844.

Syahputra, A. E., Tsau, J.-S. and B.Grigg, R. (2000), Laboratory evaluation of using lignosulfonate and surfactant mixture in co_2 flooding, 2000,. Society of Petroleum Engineers Inc., Tulsa, Oklahoma.

Todd, M. and Longstaff, W. (1972), 'The development, testing, and application of a numerical simulator for predicting miscible flood performance', *Journal of Petroleum Technology* **24**, 874–882.

Tsau, J.-S. and Heller, J. (1992), Evaluation of surfactants for co_2-foam mobility control, 1992 Copyright 1992, Society of Petroleum Engineers Inc., Midland, Texas.

Wang, J., McVay, D. A. and Ayers, W. B. (2008), Compositional simulation and optimization of secondary and tertiary recovery strategies in monument butte field, utah, Society of Petroleum Engineers, Pittsburgh, Pennsylvania, USA.

Xing, D., Wei, B., Trickett, K., Mohamed, A., Eastoe, J., Soong, Y. and Enick, R. M. (2010), co_2-soluble surfactants for improved mobility control, Society of Petroleum Engineers, Tulsa, Oklahoma, USA.

Yongmao, H., Zenggui, W., Binshan, J., Yueming, C. and Xiangjie, L. (2004), Laboratory investigation of co_2 flooding, Society of Petroleum Engineers, Abuja, Nigeria.

Zhou, D., Yan, M. and Calvin, W. M. (2012), Optimization of a mature co_2 flood - from continuous injection to wag, Society of Petroleum Engineers, Tulsa, Oklahoma, USA.

Zuta, J. and Fjelde, I. (2011), Mechanistic modeling of co_2-foam processes in fractured chalk rock: Effect of foam strength and gravity forces on oil recovery, Society of Petroleum Engineers, Kuala Lumpur, Malaysia.

Zuta, J., Fjelde, I. and Berenblyum, R. (2010), Experimental and simulation of co_2-foam flooding in fractured chalk rock at reservoir conditions: Effect of mode of injection on oil recovery, Society of Petroleum Engineers, Muscat, Oman.

Zuta, J., Fjelde, I., Berenblyum, R., Vartdal, L. H. and Ovesen, H. (2010), Modeling of transport of a co_2-foaming agent during co_2-foam processes in fractured chalk rock, Society of Petroleum Engineers, Tulsa, Oklahoma, USA.

Vitae

- Name : Najmudeen Sibaweihi
- Nationality : Ghanaian
- Date of Birth : January 24, 1984
- Email : *rabiu42000@gmail.com*
- Permanent Address : NZ 18, Kumawu-Zongo, Kumawu, Ashan Region,Ghana
- Mobile : +966540288694, +233268009099
- Academic Background : MS in Petroleum Engineering (May, 2013)
  King Fahd University of Petroleum & Minerals, Dhahran, Saudi Arabia
- : BS in Petroleum Engineering (June, 2009)
  Kwame Nkrumah University of Science and Technology, Kumasi, Ghana